

# The Ginzburg-Landau theory of flat band superconductors with quantum metric

Shuai A. Chen<sup>1,\*</sup> and K. T. Law<sup>1,†</sup>

<sup>1</sup>*Department of Physics, Hong Kong University of Science and Technology, Clear Water Bay, Hong Kong, China*  
(Dated: June 13, 2023)

Recent experimental study unveiled highly unconventional phenomena in the superconducting twisted bilayer graphene (TBG) with ultra flat bands, which cannot be described by the conventional BCS theory. For example, given the small Fermi velocity of the flat bands, the predicted superconducting coherence length according to BCS theory is more than 20 times shorter than the measured values. A new theory is needed to understand many of the unconventional properties of flat band superconductors. In this work, we establish a Ginzburg-Landau (GL) theory from a microscopic flat band Hamiltonian. The GL theory shows how the properties of the physical quantities such as the critical temperature, the superconducting coherence length, the upper critical field and the superfluid density are governed by the quantum metric of the Bloch states. One key conclusion is that the superconducting coherence length is not determined by the Fermi velocity but by the size of the optimally localized Wannier functions which is limited by quantum metric. Applying the theory to TBG, we calculated the superconducting coherence length and the upper critical fields. The results match the experimental ones well without fine tuning of parameters. The established GL theory provides a new and general theoretical framework for understanding flat band superconductors with quantum metric.

**Introduction.**— Our understanding of quantum states of matter has been greatly deepened by the study of the geometric properties of Bloch states in crystals. Specifically, the imaginary and real parts of the quantum geometric tensor of Bloch states, which are the Berry curvature and the quantum metric respectively, greatly influence the properties of the quantum state [1, 2]. The Berry curvature arises from the phase difference between two neighboring Bloch states and characterizes the band topology of states such as the quantum Hall and the Chern insulating states [2–9]. On the other hand, the quantum metric measures the distance between two adjacent Bloch states [10, 11]. It describes the wave function extension and quantifies the level of obstructions of an exponentially localized Wannier basis [2]. The quantum metric property is important for the formation of fractional quantum Hall and fractional Chern insulating states [13–19]. More recent studies have shown the fundamental roles of quantum metric in various physical phenomena, including quantum transport and electromagnetic responses [20–28], superfluidity and superconductivity in flat bands [3, 30–43], and quantum phase transitions [44–48]. In particular, the effect of quantum metric on the properties of moiré materials has attracted much attention in recent years [16, 17, 49–52, 55–62].

The quantum metric effect on superconductivity in flat band systems with vanishing Fermi velocity  $v_F$  is particularly interesting. On one hand, according to BCS theory, a large pairing gap  $\Delta$  and a high critical temperature  $T_c$  are expected due to the large density of states of flat bands. Moreover, the relation  $\xi = \frac{\hbar v_F}{\Delta}$  seemingly implies a vanishing short coherence length  $\xi$  such that electrons are tightly bound to form Cooper pairs. These BCS relations point to a very robust superconducting state in flat band superconductors. On the other hand, the diverging effective mass implies a vanishing superfluid weight  $D_s$  as  $D_s \propto 1/m^* \rightarrow 0$ . This implies the absence

of supercurrents and the absence of Meissner effect which define superconductivity. Recently, Peotta and Törmä [3] shed light on the problem by pointing out that a supercurrent is indeed achievable and the superfluid weight is proportional to the quantum metric for the flat bands [3, 30, 39].

Very recently, the superconducting properties of twisted bilayer graphene (TBG) with an extremely low Fermi velocity of  $v_F \approx 1,000\text{m/s}$  were studied experimentally. It was shown that many of the superconducting properties deviate greatly from the conventional BCS predictions [13]. For example, the coherence length is estimated to be around 2.6nm according to the BCS relation  $\xi = \frac{\hbar v_F}{\Delta}$ , which is much shorter than the estimated value of 55nm (at optimal doping) according to the upper critical measurements. Due to the large effective mass of the electrons, it is also expected that the superfluid stiffness, which is proportional  $\frac{1}{m^*}$ , is low. The Berezinskii-Kosterlitz-Thouless (BKT) transition temperature is estimated to be about 0.05K which is much lower than the measured  $T_c = 2.2\text{K}$  at optimal doping. In short, BCS relations which connect physical quantities with  $v_F$  or  $m^*$  failed to provide a proper description of superconductivity in TBG. A new theory is needed to understand flat band superconductivity.

In this work, we develop the Ginzburg-Landau (GL) theory of flat band superconductors by incorporating the quantum geometric properties of the Bloch electrons. Besides reproducing previous results concerning the BKT transition temperature [3] and the superfluid weight [3], the GL theory allows us to determine the coherence length and the upper critical field and their dependence on the quantum metric. The results are summarized in Table. I. Applying our theory to TBG with a small Fermi velocity, we estimated the coherence length, and the upper critical field which match the experimental measurements very well without the fine tuning of parameters as shown in Table. I and Fig. 1. A striking result concerning  $\xi$  is that it is independent of interaction strength at zero temperature and purely determined by the quantum metric effect (See also Eq. (21)). Contrary to the conventional understanding that a stronger interaction will bind electrons closer together to reduce the Cooper pair size (which is mea-

\* chsh@ust.hk

† phlaw@ust.hk

TABLE I. Comparison between the BCS theory and the GL theory of flat band superconductors. The results for the superfluid weight  $D_s$  at temperature  $T$ , superconducting transition temperature  $T_c$ , superconducting coherence length  $\xi$ , and upper critical field  $H_{c2}$  are summarized. The quantum metric  $\gamma_2^{ab}$  is defined in Eq. (11) and  $\bar{\gamma}_2^{ab}$  is averaged over the Brillouin zone as in Eq. (16). Here  $\Delta_0(T)$  denotes the mean-field order parameter at temperature  $T$ ,  $T_{\text{MF}}$  denotes the mean field critical temperature determined by Eq. (6),  $\mathcal{A}_{\text{uc}}$  is the area of a unit cell and  $\Phi_0 = hc/2e$  is the flux quantum. For a BCS superconductor,  $n_s$  is the superfluid density. The experimental values are adopted from Ref. 13.

	BCS	Flatband	TBG(Exp.)	Theory
$D_s$	$\frac{n_s}{m}$	$\frac{2g\Delta_0(T)}{\mathcal{A}_{\text{uc}}} \sqrt{\det(\bar{\gamma}_2^{ab})}$		
$T_c$	$1.75^{-1}g\Delta_0$	$\frac{\pi g\Delta_0(T_{\text{BKTF}})}{8\mathcal{A}_{\text{uc}}} \sqrt{\det(\bar{\gamma}_2^{ab})}$	2.2K	1.6K
$\xi$	$\frac{\hbar v_F}{g\Delta_0}$	$\sqrt{\frac{T_{\text{MF}}}{ T-T_{\text{MF}} }} [\det(\bar{\gamma}_2^{ab})]^{-\frac{1}{4}}$	55nm	35nm
$H_{c2}$	$2\pi(\frac{T_c}{v_F})^2$	$\frac{ T-T_{\text{MF}} }{T_{\text{MF}}} \frac{\Phi_0}{2\pi\sqrt{\det(\bar{\gamma}_2^{ab})}}$	0.10T	0.26T

sured by  $\xi$ ), the quantum metric limits the size of the Cooper pairs. The Cooper pair size cannot be smaller than the size of optimally localized Wannier functions [2] constructed by the Bloch states. In the case of TBG, the quantum metric limits  $\xi$  to be tens of nanometers as observed in the experiment [13].

In the following, we first derive the GL free energy which incorporates the quantum geometry effects of Bloch electrons. Second, the superfluid weight, the upper critical field and the superconducting coherence length are derived. Finally, we apply the GL theory to explain the unconventional behaviors of superconducting TBG.

**The Ginzburg-Landau Free Energy.**— We start with a model Hamiltonian  $H = H_0 + H_{\text{int}}$  defined on a lattice containing  $N$  sites. It is assumed that  $H_0$  possesses an isolated flat band at the Fermi energy. In general, the flat band has Bloch states which take the form  $e^{-i\mathbf{k}\cdot\mathbf{r}}g_{\mathbf{k}\xi}(\alpha)$ , where  $\alpha$  indexes the orbital degrees of freedom. Even though the band is completely flat, there can be nontrivial quantum geometry effects encoded by  $g_{\mathbf{k}\xi}(\alpha)$ . An example of a nontrivial flat band is a band with a none zero Chern number for which it is not possible to find a complete set of exponentially localized Wannier basis [2]. The occurrence of a superconducting phase is associated with the presence of an attractive interaction in a  $d$ -spatial dimensions,

$$H_{\text{int}} = -g \int d\mathbf{r} a_{\pm}^{\dagger}(\mathbf{r}) a_{\mp}^{\dagger}(\mathbf{r}) a_{-}(\mathbf{r}) a_{+}(\mathbf{r}), \quad (1)$$

with  $a_{\xi}(\mathbf{r})$  as the electron annihilation operator carrying two flavors  $\xi = \pm$ . To resolve the role of quantum geometry with interactions, we project the electron operators to the Bloch electrons of the targeted flat band

$$a_{\xi}(\mathbf{r}) \rightarrow \frac{1}{\sqrt{N}} \sum_{\mathbf{q}} e^{i\mathbf{q}\cdot\mathbf{r}} g_{\mathbf{q}\xi}^*(\alpha) c_{\mathbf{q}\xi}, \quad (2)$$

where  $c_{\mathbf{q}\xi}$  annihilates an electron with momentum  $\mathbf{q}$  over the first Brillouin on the targeted band and  $\alpha$  represents other

quantum numbers of the Bloch state. The expansion in Eq. (2) projects out other bands while  $g_{\mathbf{k}\xi}$  encodes the quantum geometry effect [64, 65]. We proceed with the Hubbard-Stratonovich transformation by introducing a bosonic field  $\Delta(\mathbf{r})$ ,

$$\Delta(\mathbf{r}) = a_{-}(\mathbf{r})a_{+}(\mathbf{r}), \quad (3)$$

Then, the Lagrangian density  $\mathcal{L}$  is obtained through the path integral approach (see Supplementary Materials(SM) [66]) such that

$$\mathcal{L} = (-i\omega - \mu)(\bar{c}_{\mathbf{k},+}c_{\mathbf{k},+} + \bar{c}_{\mathbf{k},-}c_{\mathbf{k},-}) - g \sum_{\mathbf{q}} [\Gamma(\mathbf{q}, \mathbf{k})\Delta(\mathbf{k})\bar{c}_{\mathbf{q}+\frac{\mathbf{k}}{2},+}\bar{c}_{-\mathbf{q}+\frac{\mathbf{k}}{2},-} + h.c.], \quad (4)$$

where  $c_{\mathbf{q},\xi}$  denotes the Grassmann fields,  $\mu$  is the chemical potential and  $\Delta(\mathbf{k}) \equiv \sum_{\mathbf{r}} \Delta(\mathbf{r})e^{i\mathbf{k}\cdot\mathbf{r}}$  is the Fourier component of the bosonic field  $\Delta(\mathbf{r})$ . The projection in Eq. (2) introduces the form factor  $\Gamma(\mathbf{q}, \mathbf{k})$  that modifies the coupling constant  $g$ . The form factor is defined as  $\Gamma(\mathbf{q}, \mathbf{k}) \equiv \sum_{\alpha} g_{-\mathbf{q}+\mathbf{k}/2,+}(\alpha)g_{\mathbf{q}+\mathbf{k}/2,-}(\alpha)$ , and it plays a crucial role in the context of superconductivity. Formally, the GL free energy  $F[\Delta]$  is obtained by integrating out the fermion fields at a finite temperature  $T$  such that,

$$F[\Delta] = \sum_{\mathbf{k}} g\bar{\Delta}(\mathbf{k})\Delta(\mathbf{k}) - T \ln \int \mathcal{D}[c, \bar{c}] e^{-\int_0^{\beta} d\tau \sum_{\mathbf{q}} \mathcal{L}}. \quad (5)$$

To calculate  $F[\Delta]$ , we perform an expansion  $\Delta(\mathbf{k}) = \Delta_0\delta_{\mathbf{k},0} + \delta\Delta(\mathbf{k})$  around the extremum of  $F[\Delta]$ . Here,  $\Delta_0$  represents the mean-field value at temperature  $T$ , while  $\delta\Delta(\mathbf{k})$  represents the fluctuations of the order parameter. By minimizing the GL free energy  $\frac{\partial F[\Delta]}{\partial \Delta_0} = \frac{\partial F[\Delta]}{\partial \delta\Delta_0} = 0$ , the mean field order parameter  $\Delta_0$  can be determined from the self-consistent gap equation

$$1 = \frac{1}{N} \sum_{\mathbf{q}} \frac{g|\Gamma(\mathbf{q})|^2}{2\epsilon(\mathbf{q})} \tanh \frac{\beta\epsilon(\mathbf{q})}{2}, \quad (6)$$

where  $\epsilon(\mathbf{q}) = \sqrt{|g\Gamma(\mathbf{q})\Delta_0|^2 + \mu^2}$  denotes the dispersion of Bogoliubov quasiparticles. In the presence of time-reversal symmetry  $g_{-\mathbf{k},-} = g_{\mathbf{k},+}^*$ ,  $\Gamma(\mathbf{q}) = 1$  and under a uniform ansatz  $\Delta(\mathbf{r}) = \Delta_0$ , from Eq. (6) one may extract a relation  $g\Delta_0/T_{\text{MF}} = 2$  at half-filling with  $T_{\text{MF}}$  as the critical temperature and  $g\Delta_0$  as the pairing gap (see SM [66]), which is larger than the ratio ( $\sim 1.7$ ) from a conventional BCS theory.

Going beyond mean field and include the fluctuations, we have  $F[\Delta] = F_0 + F_2 + \mathcal{O}(|\delta\Delta|^4)$  up to the second order of  $\delta\Delta(\mathbf{k})$ . In particular,  $F_0$  recovers the grand potential

$$F_0 = \sum_{\mathbf{k}} \left[ g|\Delta_0|^2 - 2\ln(1 + e^{-\beta\epsilon(\mathbf{k})}) + \epsilon(\mathbf{k}) \right]. \quad (7)$$

The second order  $F_2 \equiv \sum_{\mathbf{k}} \mathcal{L}[\delta\Delta]$  describes the Gaussian

fluctuations with

$$\mathcal{L}[\delta\Delta] = [g - g^2\chi(\mathbf{k})] \delta\bar{\Delta}(\mathbf{k})\delta\Delta(\mathbf{k}), \quad (8)$$

where  $\chi(\mathbf{k})$  is the four-point correlation function,

$$\begin{aligned} \chi(\mathbf{k}) \equiv & \frac{1}{N} \sum_q |\Gamma(\mathbf{q}, \mathbf{k})|^2 [\mathcal{G}(q + k/2)\mathcal{G}(-q + k/2) \\ & + \mathcal{F}(q + k/2)\mathcal{F}(-q + k/2)], \end{aligned} \quad (9)$$

with Gor'kov's normal and anomalous Green functions  $\mathcal{G}(q)$  and  $\mathcal{F}(q)$  ( $q = (\mathbf{q}, \omega)$ ) (see SM [66]). In contrast to conventional superconductors, the Bloch wavefunctions play a significant role in both the effective interaction and the quasiparticle dispersion. The prefactor  $|\Gamma(\mathbf{q}, \mathbf{k})|^2$  in Eq. (9) highlights the importance of the wavefunctions of the Bloch wavefunctions. The significance of  $|\Gamma(\mathbf{q}, \mathbf{k})|^2$  is that, the pairing strength of a finite momentum Cooper pair is weighed by  $\Gamma(\mathbf{q}, \mathbf{k})$ , such that  $\chi(\mathbf{k})$  is  $\mathbf{k}$ -dependent. This generates a finite superfluid weight to account for the Meissner effect, even though the effective mass of electrons diverges for a completely flat band. As we show below, the form factor encodes the quantum metric effects.

*Superfluid weight, BKT transition and quantum metric.*—

In general, the form factor can be expanded as a function of  $\mathbf{k}$  up to the second order:

$$|\Gamma(\mathbf{q}, \mathbf{k})|^2 = \gamma_0(\mathbf{q}) - \sum_{ab} \gamma_2^{ab}(\mathbf{q}) k_a k_b, \quad (10)$$

where the absence of a linear term is due to the stability of the mean-field ansatz.

For the time-reversal invariant system where  $g_{\mathbf{q},+} = g_{\mathbf{q},-}^* \equiv g_{\mathbf{q}}$ ,  $\gamma_0(\mathbf{q})$  becomes the inner product  $\gamma_0(\mathbf{q}) \equiv |\langle g_{\mathbf{q}} | g_{\mathbf{q}} \rangle|^2 = 1$  and  $\gamma_2(\mathbf{q})$  is the Fubini-Study metric [1, 67] with components

$$\gamma_2^{ab}(\mathbf{q}) \equiv \text{Re} \langle \partial_{\mathbf{q}_a} g_{\mathbf{q}} | (1 - |g_{\mathbf{q}}\rangle\langle g_{\mathbf{q}}|) | \partial_{\mathbf{q}_b} g_{\mathbf{q}} \rangle, \quad (11)$$

which measures the Bures distance between two quantum states. The quantum metric  $\gamma_2^{ab}(\mathbf{q})$  characterizes how the Bloch states interfere with each other. The appearance of the quantum metric in Eq. (9) and Eq. (10) clearly illustrates the crucial role of the quantum geometric effect in determining superconductivity fluctuations. In contrast, this effect is not evident at the mean-field level, as demonstrated by Eq. (7). After integrating out the Matsubara frequency along with the expansion in Eq. (10), we have  $\chi(\mathbf{k}) = \chi_0 - \frac{1}{8} \sum_{ab} \chi_2^{ab} k_a k_b$ , with the explicit form as

$$\chi_0 = \frac{1}{N} \sum_{\mathbf{q}} \frac{\gamma_0(\mathbf{q})}{2} \frac{1}{\epsilon(\mathbf{q})}, \quad (12)$$

$$\chi_2^{ab} = \frac{2g^2\Delta_0^2}{N} \sum_{\mathbf{q}} \frac{\tanh\left(\frac{\beta\epsilon(\mathbf{q})}{2}\right)}{\epsilon(\mathbf{q})} \gamma_2^{ab}(\mathbf{q}). \quad (13)$$

Thus in the continuum limit  $F_2 = \int d^d\mathbf{r} \mathcal{L}[\delta\Delta]$ , we reach an

effective theory  $\mathcal{L}[\delta\Delta]$

$$\mathcal{L}[\delta\Delta] = \frac{1}{8} \sum_{ab} D_s^{ab} \partial_a \delta\bar{\Delta} \partial_b \delta\Delta. \quad (14)$$

The presence of the factor  $D_s^{ab} \equiv \mathcal{A}_{\text{uc}}^{-1} \chi_s^{ab}$ , with  $\mathcal{A}_{\text{uc}}$  being area of the unit cell, which depends on  $\gamma_2^{ab}(\mathbf{q})$ , indicates that the dynamics of the fluctuation of the order parameter is governed by the quantum geometry. The superfluid weight is measured by the factor  $\gamma_2^{ab}(\mathbf{q})$ . Conversely, in the absence of quantum geometry ( $\gamma_2^{ab} = 0$ ), as indicated by  $D_s^{ab} = 0$  in Eq. (14), there will be no fluctuations. Examine the phase fluctuations  $\delta\Delta(\mathbf{r}) = \Delta_0 e^{2i\theta(\mathbf{r})} - \Delta_0 \simeq 2i\theta(\mathbf{r})\Delta_0$  (and ignore the amplitude fluctuations), and we obtain the effective Lagrangian

$$\mathcal{L}[\theta] = \frac{1}{2} \sum_{ab} D_s^{ab} \partial_a \theta \partial_b \theta, \quad (15)$$

and the supercurrent  $j_b = \sum_a D_s^{ab} \partial_a \theta$ . We can now determine the BKT transition temperature  $T_{\text{BKT}} = \pi \sqrt{\det D_s^{ab}} / 8$  [68], by identifying the factor  $D_s^{ab}$  in Eq. (13) as the intrinsic superfluid weight, which is consistent with previous studies [3, 30, 39]. Basically, the order parameter  $\Delta_0$  depends on temperature  $T$ , and thus  $T_{\text{BKT}}$  should be solved self-consistently. For an isotropic superconductor with a flat Bogoliubov quasiparticle band, a simple relation  $T_{\text{BKT}}/g\Delta_0 = \frac{\pi \sqrt{\det \bar{\gamma}_2^{ab}}}{8\mathcal{A}_{\text{uc}}}$  holds around filling  $\mu = 0$ , where the average of the quantum metric over the Brillouin zone is:

$$\bar{\gamma}_2^{ab} = \frac{1}{N} \sum_{\mathbf{q}} \gamma_2^{ab}(\mathbf{q}). \quad (16)$$

Interesting, when the  $\bar{\gamma}_2^{ab}$  is tuned to be sufficiently large,  $T_{\text{BKT}}$  will approaches to  $T_{\text{MF}}$  that is obtained from Eq. (6) (see SM [66]). It is important to emphasize that in conventional superconductors,  $D_s = n_s/m^*$  with  $n_s$  being the superfluid density at temperature  $T$ , such that  $T_{\text{BKT}} = \pi n_s / (8m^*)$  which goes to zero for flat bands.

*Upper critical field  $H_{c2}$ .*— Another important physical quantity of a superconductor is the (orbital) upper critical field which is expected to be infinite according to BCS theory for a flat band. As the mean-field order parameter is suppressed by vortex excitations around  $H_{c2}$ , we can derive the GL free energy from Eq. (5) by assuming a vanishing mean field,  $\Delta_0 = 0$ . An effective Lagrangian can be obtained after integrating out the fermion field, and for an isotropic system, we have in the continuum limit  $F_2 = \int d^d\mathbf{r} \mathcal{L}[\delta\Delta]$ ,

$$\mathcal{L}[\delta\Delta] = \frac{1}{2m^*} |\nabla\delta\Delta|^2 + a(T) |\delta\Delta|^2 + \mathcal{O}(|\delta\Delta|^4), \quad (17)$$

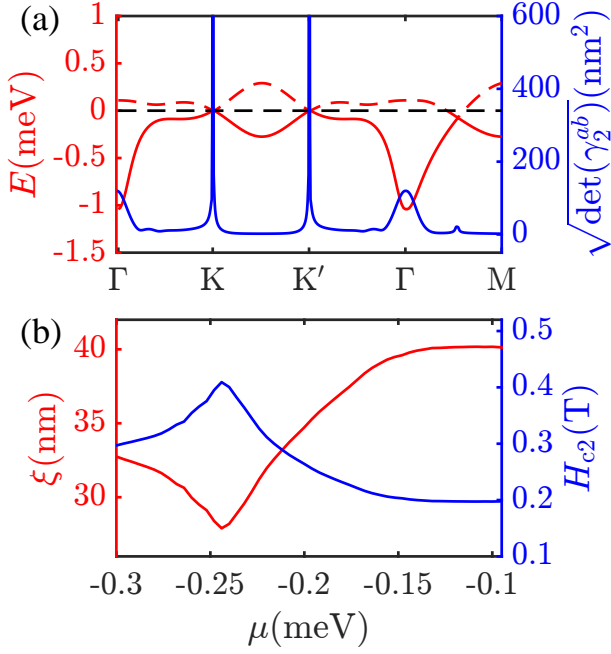


FIG. 1. (a) The band structure and distribution of the quantum metric  $\sqrt{\det(\bar{\gamma}_2^{ab})}$ , as shown in Eq. (11), over the moiré BZ in a TBG. The quantum metric diverges at the two Dirac points at K and K', while it significantly contributes at  $\Gamma$ . (b) The superconducting coherence length  $\xi$  as a function of chemical potential  $\mu$  in the low-temperature limit. Initially, as doping moves away from  $\mu = -0.1$  meV,  $\xi$  decreases, but it then increases around  $\mu = -0.3$  meV. Our calculations use a temperature of  $\beta = 200$  meV $^{-1}$ , and we only display one spin-valley species for simplification.

with

$$\frac{1}{2m^*} = \frac{\beta g^2 \bar{\nu}}{4\mathcal{A}_{uc}} \sqrt{\det(\bar{\gamma}_2^{ab})}, \quad (18)$$

$$a(T) = \frac{4g - g^2 \beta \bar{\nu} \bar{\gamma}_0}{4\mathcal{A}_{uc}}, \quad (19)$$

where  $\bar{\gamma}_0 = \frac{1}{N} \sum_{\mathbf{q}} \gamma_0(\mathbf{q})$  and  $\bar{\nu} = \frac{2(1-2\nu)}{\ln(\nu^{-1}-1)}$  with  $\nu$  being the filling factor. *Hereafter*, we focus on a system of time reversal symmetry to simply have  $\bar{\gamma}_0 = 1$ . We discover that the quantum metric  $\sqrt{\det(\bar{\gamma}_2^{ab})}$  gives rise to a finite effective mass of Cooper pairs, whereas the change in sign of  $a(T)$  gives rise to the mean field critical temperature  $T_{MF} = g\frac{\bar{\nu}}{4}$ . The magnetic field can be included in the free energy by the minimal coupling  $-i\nabla \rightarrow -i\nabla + 2e\mathbf{A}$  in Eq. (17). Then, the upper critical field  $H_{c2}$  can be determined using the standard GL approach [1] and we have:

$$H_{c2} = \frac{\Phi_0}{2\pi \sqrt{\det(\bar{\gamma}_2^{ab})}} \frac{|T - T_{MF}|}{T_{MF}}. \quad (20)$$

where  $\Phi_0 = hc/2e$  is a flux quantum. It is clear that a finite average quantum metric  $\bar{\gamma}_2^{ab}$  gives rise to a finite  $H_{c2}$ . From the inequality,  $\sqrt{\det(\bar{\gamma}_2^{ab}(\mathbf{k}))} \geq \frac{1}{2} |\text{Tr}\mathcal{B}(\mathbf{k})|$  for

two dimensional systems [1, 3], we have  $\sqrt{\det(\bar{\gamma}_2^{ab})} \geq 1/N \sum_{\mathbf{q}} \sqrt{\det(\bar{\gamma}_2^{ab})} \geq 1/N \sum_{\mathbf{q}} \frac{1}{2} |\text{Tr}\mathcal{B}(\mathbf{k})| \geq \mathcal{A}_{uc} \frac{|C|}{2\pi}$ , where  $\mathcal{B}(\mathbf{k})$  is the Berry curvature and  $C$  is the Chern number. This leads to two important observations. First, the upper critical field  $H_{c2}$  is bound by  $H_{c2} \leq \frac{\Phi_0}{\mathcal{A}_{uc}|C|} \frac{|T - T_{MF}|}{T_{MF}}$  for a topological band. Second, even for a topological trivial band, as long as the Berry curvature is locally finite, the quantum geometry is relevant and is bounded by the averaged  $|\text{Tr}\mathcal{B}(\mathbf{k})|$ . Moreover, using the condition  $H_{c2}\xi^2 = \Phi_0/2\pi$ , we find that the superconducting coherence length to be :

$$\xi = \sqrt{\frac{T_{MF}}{|T - T_{MF}|}} [\det(\bar{\gamma}_2^{ab})]^{\frac{1}{4}}. \quad (21)$$

As expected, the expression of  $\xi$  is dramatically different from the BCS relation  $\xi = \frac{\hbar v_F}{\Delta}$  which vanishes as  $v_F$  goes to zero. It is important to note that at zero temperature, the coherence length is reduced to  $\xi(T=0) = [\det(\bar{\gamma}_2^{ab})]^{\frac{1}{4}}$  which is the size of optimally localized wannier functions constructed from the Bloch states of the flat band [2, 3] (also see SM [66]). This is a very interesting result that  $\xi$  is the shortest at  $T = 0$  and independent of the interaction strength  $g$ . It means that the minimal Cooper pair size is purely determined by the quantum metric and a stronger interaction cannot bound the electrons closer to each other. When temperature increases, the interaction energy is incorporated into  $T_{MF}$  and affects  $\xi$ .

**Application to TBG**—Recently, superconductivity was observed in TBG with extremely small  $v_F$ , estimated to be around 1,000m/s. In this section, we employ the GL theory developed above to explain the observed superconducting coherence length which is about 20 times larger than the one estimated from BCS theory.

As shown in Eq. (21), to calculate the coherence length  $\xi$  at zero temperature, we calculate the quantum metric of the Bloch states of the flat bands using the Bistritzer-Macdonald model to describe the moiré band structure of TBG near the magic angle [14]. The details of the model is given in the SM [66]. In Fig. 1(a), the band structure at twisted angle  $\theta = 1.08^\circ$  is shown and the bandwidth is extremely narrow which is on the order of 1meV. For simplicity, only the moiré bands originated from one valley is shown.

It is clear that the valence (solid line) and the conduction (dashed line) bands touch at the Dirac points at K and K' of the moiré Brillouin zone. Here, the energy at the Dirac points is set to have chemical potential  $\mu = 0$ , corresponding to the filling factor of  $\nu = 0$ . To model the superconducting phase, we assume a simple singlet pairing potential [16, 17]  $H_{int} = -g \int d^2\mathbf{r} \sum_{\ell\xi} \psi_{\uparrow\rho,\ell\xi}^\dagger(\mathbf{r}) \psi_{\downarrow\bar{\rho},\ell\xi}^\dagger(\mathbf{r}) \psi_{\downarrow\bar{\rho},\ell\xi}(\mathbf{r}) \psi_{\uparrow\rho,\ell\xi}(\mathbf{r})$  with the valley indices  $\rho = \pm$ , sublattices  $\xi = A, B$ , and layer  $\ell$ , while ignoring other correlation effects induced by interactions between electrons [49, 71]. Here  $\psi_{\sigma\rho,\ell\xi}$  denotes the Fermion operators in the continuum limit. It is important to note that the pairing needs not be in this form in TBG but we focus on the quantum metric effect here regardless of the details of the pairing.

We can determine the superconducting coherence length within the GL theory using Eq. (21). At the low temperature

limit  $\beta \rightarrow \infty$ , the coherence length originating from quantum metric is essentially determined by the quantum metric  $\xi = [(\det \gamma_2^{ab})]^{1/4}$ , which is independent of the pairing coupling  $g$ . The quantum metric as a function of momentum is shown in Fig. 1(a). It is interesting to note that the quantum metric diverges around the two Dirac points and takes a relatively large value at  $\Gamma$ . When evaluating the coherence length  $\xi$ , we take into account the finite bandwidth of TBG in Eq. (9) and the details are shown in SM [66]. Fig. 1(b) shows the variation of  $\xi$  with different chemical potentials  $\mu$  which is relevant to the experimental regime where the filling factor is below  $-1/2$  at  $\mu = -0.12\text{meV}$ . In the regime  $-0.28\text{meV} < \mu < -0.2\text{meV}$ , we see a decrease and then increase of  $\xi$  as the chemical potential lowers. The increase of  $\xi$  at lower chemical potential is due to the increase of quantum metric near the  $\Gamma$ -point of the model. Amazingly, similar  $\xi$  dependence on the chemical potential was observed in the experiment [13]. Without fine tuning of parameters, we obtained  $\xi \approx 30\text{nm}$  at zero temperature which is comparable with the experimental values of about  $55\text{nm}$ . The estimated  $H_{c2}$  are also plotted in Fig. 1(b). The optimal  $H_{c2} \sim 0.26\text{T}$  which is comparable with the experimental value of  $0.1\text{T}$ . It is important to note that the deviation of the theoretical results at  $T = 0$  from the experimental results can be due to the finite

temperature effects which increase  $\xi$  and reduce  $H_{c2}$ .

**Conclusion.**— We developed a GL theory for flat band superconductors which includes the quantum metric effects. The GL theory allows us to derive many of the important physical quantities of superconductors in terms of the quantum metric of the Bloch electrons as summarized in Table I. Importantly, we found that the coherence length, which is expected to be zero from conventional BCS theory, is finite for flat bands with quantum metric. Physically, the size of the optimally localized Wannier functions, which is governed by the quantum metric, determines the superconducting coherence length at zero temperature. By calculating the quantum metric of TBG, we explained the coherence length dependence on the charge density in the experiment. This GL theory provides a general framework to understand the unconventional properties of flat band superconductors with quantum metric.

**Acknowledgments.**— We thank Jeanie Lau for informing us their experimental results which inspired this work. We acknowledge valuable discussions with Tai-Kai Ng, Adrian Po, Wen Huang and Yan-bin Yang. K.T.L. acknowledges the support of the Ministry of Science and Technology, China, and the Hong Kong Research Grants Council through Grants No. 2020YFA0309600, No. RFS2021-6S03, No. C6025-19G, No. AoE/P-701/20, No. 16310520, No. 16310219, No. 16307622, and No. 16309718.

- 
- [1] J. P. Provost and G. Vallee, Riemannian structure on manifolds of quantum states, *Communications in Mathematical Physics* **76**, 289 (1980).
- [2] M. V. Berry, The quantum phase, five years after, in *Geometric phases in physics*, edited by A. Shapere and F. Wilczek (World scientific, Singapore, 1989) Chap. 1, pp. 1–28.
- [3] K. v. Klitzing, G. Dorda, and M. Pepper, New method for high-accuracy determination of the fine-structure constant based on quantized hall resistance, *Phys. Rev. Lett.* **45**, 494 (1980).
- [4] D. J. Thouless, M. Kohmoto, M. P. Nightingale, and M. den Nijs, Quantized hall conductance in a two-dimensional periodic potential, *Phys. Rev. Lett.* **49**, 405 (1982).
- [5] M. V. Berry, Quantal Phase Factors Accompanying Adiabatic Changes, *Proceedings of the Royal Society of London Series A* **392**, 45 (1984).
- [6] J. Bellissard, A. van Elst, and H. Schulz-Baldes, The noncommutative geometry of the quantum Hall effect, *Journal of Mathematical Physics* **35**, 5373 (1994), arXiv:cond-mat/9411052 [cond-mat].
- [7] M. Z. Hasan and C. L. Kane, Colloquium: Topological insulators, *Rev. Mod. Phys.* **82**, 3045 (2010).
- [8] X.-L. Qi and S.-C. Zhang, Topological insulators and superconductors, *Rev. Mod. Phys.* **83**, 1057 (2011).
- [9] A. Bouhon, A. Timmel, and R.-J. Slager, Quantum geometry beyond projective single bands, arXiv e-prints , arXiv:2303.02180 (2023), arXiv:2303.02180 [cond-mat.mes-hall].
- [10] J. Anandan and Y. Aharonov, Geometry of quantum evolution, *Phys. Rev. Lett.* **65**, 1697 (1990).
- [11] R. Resta, The insulating state of matter: a geometrical theory, *European Physical Journal B* **79**, 121 (2011), arXiv:1012.5776 [cond-mat.mtrl-sci].
- [12] N. Marzari and D. Vanderbilt, Maximally localized generalized wannier functions for composite energy bands, *Phys. Rev. B* **56**, 12847 (1997).
- [13] F. D. M. Haldane, Geometrical description of the fractional quantum hall effect, *Phys. Rev. Lett.* **107**, 116801 (2011).
- [14] S. M. Girvin, A. H. MacDonald, and P. M. Platzman, Magneto-roton theory of collective excitations in the fractional quantum hall effect, *Phys. Rev. B* **33**, 2481 (1986).
- [15] M. M. Fogler, Stripe and Bubble Phases in Quantum Hall Systems, in *High Magnetic Fields*, Vol. 595, edited by C. Berthier, L. P. Lévy, and G. Martinez (2002) pp. 98–138.
- [16] S. A. Parameswaran, R. Roy, and S. L. Sondhi, Fractional quantum Hall physics in topological flat bands, *Comptes Rendus Physique* **14**, 816 (2013), arXiv:1302.6606 [cond-mat.str-el].
- [17] E. Dobardžić, M. V. Milovanović, and N. Regnault, Geometrical description of fractional chern insulators based on static structure factor calculations, *Phys. Rev. B* **88**, 115117 (2013).
- [18] R. Roy, Band geometry of fractional topological insulators, *Phys. Rev. B* **90**, 165139 (2014).
- [19] J. Wang, S. Klevtsov, and Z. Liu, Origin of Model Fractional Chern Insulators in All Topological Ideal Flatbands: Explicit Color-entangled Wavefunction and Exact Density Algebra, arXiv e-prints , arXiv:2210.13487 (2022), arXiv:2210.13487 [cond-mat.mes-hall].
- [20] T. Neupert, C. Chamon, and C. Mudry, Measuring the quantum geometry of bloch bands with current noise, *Phys. Rev. B* **87**, 245103 (2013).
- [21] A. Srivastava and A. m. c. Imamoğlu, Signatures of bloch-band geometry on excitons: Nonhydrogenic spectra in transition-metal dichalcogenides, *Phys. Rev. Lett.* **115**, 166802 (2015).
- [22] Y. Gao, S. A. Yang, and Q. Niu, Field induced positional shift of bloch electrons and its dynamical implications, *Phys. Rev.*

- Lett.* **112**, 166601 (2014).
- [23] F. Piéchon, A. Raoux, J.-N. Fuchs, and G. Montambaux, Geometric orbital susceptibility: Quantum metric without berry curvature, *Phys. Rev. B* **94**, 134423 (2016).
- [24] W. Chen and W. Huang, Quantum-geometry-induced intrinsic optical anomaly in multiorbital superconductors, *Phys. Rev. Research* **3**, L042018 (2021).
- [25] J. Ahn and N. Nagaosa, Superconductivity-induced spectral weight transfer due to quantum geometry, *Phys. Rev. B* **104**, L100501 (2021).
- [26] V. Kozii, A. Avdoshkin, S. Zhong, and J. E. Moore, Intrinsic anomalous hall conductivity in a nonuniform electric field, *Phys. Rev. Lett.* **126**, 156602 (2021).
- [27] J. Ahn, G.-Y. Guo, N. Nagaosa, and A. Vishwanath, Riemannian geometry of resonant optical responses, *Nature Physics* **18**, 290 (2021), arXiv:2103.01241 [cond-mat.mes-hall].
- [28] J. Mitscherling and T. Holder, Bound on resistivity in flat-band materials due to the quantum metric, *Phys. Rev. B* **105**, 085154 (2022), arXiv:2110.14658 [cond-mat.mes-hall].
- [3] S. Peotta and P. Törmä, Superfluidity in topologically nontrivial flat bands, *Nature Communications* **6**, 8944 (2015), arXiv:1506.02815 [cond-mat.supr-con].
- [30] L. Liang, T. I. Vanhala, S. Peotta, T. Siro, A. Harju, and P. Törmä, Band geometry, berry curvature, and superfluid weight, *Phys. Rev. B* **95**, 024515 (2017).
- [31] M. Iskin, Quantum-metric contribution to the pair mass in spin-orbit-coupled fermi superfluids, *Phys. Rev. A* **97**, 033625 (2018).
- [32] P. Törmä, L. Liang, and S. Peotta, Quantum metric and effective mass of a two-body bound state in a flat band, *Phys. Rev. B* **98**, 220511 (2018).
- [33] M. Jip Park, Y. B. Kim, and S. Lee, Geometric Superconductivity in 3D Hofstadter Butterfly, arXiv e-prints , arXiv:2007.16205 (2020), arXiv:2007.16205 [cond-mat.supr-con].
- [34] J. S. Hofmann, E. Berg, and D. Chowdhury, Superconductivity, pseudogap, and phase separation in topological flat bands, *Phys. Rev. B* **102**, 201112 (2020).
- [35] M. Iskin, Collective excitations of a bcs superfluid in the presence of two sublattices, *Phys. Rev. A* **101**, 053631 (2020).
- [36] A. Julku, S. Peotta, T. I. Vanhala, D.-H. Kim, and P. Törmä, Geometric origin of superfluidity in the lieb-lattice flat band, *Phys. Rev. Lett.* **117**, 045303 (2016).
- [37] A. Julku, G. M. Bruun, and P. Törmä, Quantum geometry and flat band bose-einstein condensation, *Phys. Rev. Lett.* **127**, 170404 (2021).
- [38] J. Herzog-Arbeitman, V. Peri, F. Schindler, S. D. Huber, and B. A. Bernevig, Superfluid weight bounds from symmetry and quantum geometry in flat bands, *Phys. Rev. Lett.* **128**, 087002 (2022).
- [39] K.-E. Huhtinen, J. Herzog-Arbeitman, A. Chew, B. A. Bernevig, and P. Törmä, Revisiting flat band superconductivity: Dependence on minimal quantum metric and band touchings, *Phys. Rev. B* **106**, 014518 (2022).
- [40] X. Hu, T. Hyart, D. I. Pikulin, and E. Rossi, Quantum-metric-enabled exciton condensate in double twisted bilayer graphene, *Phys. Rev. B* **105**, L140506 (2022).
- [41] S. M. Chan, B. Grémaud, and G. G. Batrouni, Designer flat bands: Topology and enhancement of superconductivity, *Phys. Rev. B* **106**, 104514 (2022).
- [42] J. Herzog-Arbeitman, A. Chew, K.-E. Huhtinen, P. Törmä, and B. A. Bernevig, Many-Body Superconductivity in Topological Flat Bands, arXiv e-prints , arXiv:2209.00007 (2022), arXiv:2209.00007 [cond-mat.str-el].
- [43] J. S. Hofmann, E. Berg, and D. Chowdhury, Superconductivity, charge density wave, and supersolidity in flat bands with tunable quantum metric, arXiv e-prints , arXiv:2204.02994 (2022), arXiv:2204.02994 [cond-mat.str-el].
- [44] T. Thonhauser and D. Vanderbilt, Insulator/Chern-insulator transition in the Haldane model, *Phys. Rev. B* **74**, 235111 (2006), arXiv:cond-mat/0608527 [cond-mat.mes-hall].
- [45] L. Campos Venuti and P. Zanardi, Quantum critical scaling of the geometric tensors, *Phys. Rev. Lett.* **99**, 095701 (2007).
- [46] P. Zanardi, P. Giorda, and M. Cozzini, Information-theoretic differential geometry of quantum phase transitions, *Phys. Rev. Lett.* **99**, 100603 (2007).
- [47] N. Verma, T. Hazra, and M. Randeria, Optical spectral weight, phase stiffness, and  $T_c$  bounds for trivial and topological flat band superconductors, *Proceedings of the National Academy of Science* **118**, e2106744118 (2021), arXiv:2103.08540 [cond-mat.supr-con].
- [48] D. Mao and D. Chowdhury, Diamagnetic response and phase stiffness for interacting isolated narrow bands, *Proceedings of the National Academy of Science* **120**, e2217816120 (2023), arXiv:2209.06817 [cond-mat.str-el].
- [49] Y. Cao, V. Fatemi, A. Demir, S. Fang, S. L. Tomarken, J. Y. Luo, J. D. Sanchez-Yamagishi, K. Watanabe, T. Taniguchi, E. Kaxiras, R. C. Ashoori, and P. Jarillo-Herrero, Correlated insulator behaviour at half-filling in magic-angle graphene superlattices, *Nature (London)* **556**, 80 (2018), arXiv:1802.00553 [cond-mat.mes-hall].
- [50] Y. Cao, V. Fatemi, S. Fang, K. Watanabe, T. Taniguchi, E. Kaxiras, and P. Jarillo-Herrero, Unconventional superconductivity in magic-angle graphene superlattices, *Nature (London)* **556**, 43 (2018), arXiv:1803.02342 [cond-mat.mes-hall].
- [51] X. Lu, P. Stepanov, W. Yang, M. Xie, M. A. Aamir, I. Das, C. Urgell, K. Watanabe, T. Taniguchi, G. Zhang, A. Bachtold, A. H. MacDonald, and D. K. Efetov, Superconductors, orbital magnets and correlated states in magic-angle bilayer graphene, *Nature (London)* **574**, 653 (2019), arXiv:1903.06513 [cond-mat.str-el].
- [52] T. Hazra, N. Verma, and M. Randeria, Bounds on the superconducting transition temperature: Applications to twisted bilayer graphene and cold atoms, *Phys. Rev. X* **9**, 031049 (2019).
- [17] X. Hu, T. Hyart, D. I. Pikulin, and E. Rossi, Geometric and conventional contribution to the superfluid weight in twisted bilayer graphene, *Phys. Rev. Lett.* **123**, 237002 (2019).
- [16] A. Julku, T. J. Peltonen, L. Liang, T. T. Heikkilä, and P. Törmä, Superfluid weight and berezinskii-kosterlitz-thouless transition temperature of twisted bilayer graphene, *Phys. Rev. B* **101**, 060505 (2020).
- [55] P. J. Ledwith, G. Tarnopolsky, E. Khalaf, and A. Vishwanath, Fractional chern insulator states in twisted bilayer graphene: An analytical approach, *Phys. Rev. Research* **2**, 023237 (2020).
- [56] F. Xie, Z. Song, B. Lian, and B. A. Bernevig, Topology-Bounded Superfluid Weight in Twisted Bilayer Graphene, *Phys. Rev. Lett.* **124**, 167002 (2020), arXiv:1906.02213 [cond-mat.supr-con].
- [57] S. Chaudhary, C. Lewandowski, and G. Refael, Shift-current response as a probe of quantum geometry and electron-electron interactions in twisted bilayer graphene, *Phys. Rev. Research* **4**, 013164 (2022).
- [58] B. Mera and T. Ozawa, Engineering geometrically flat chern bands with fubini-study kähler structure, *Phys. Rev. B* **104**, 115160 (2021).
- [59] D. Kaplan, T. Holder, and B. Yan, Twisted photovoltaics at terahertz frequencies from momentum shift current, *Phys. Rev. Research* **4**, 013209 (2022).

- [60] P. Törmä, S. Peotta, and B. A. Bernevig, Superfluidity and Quantum Geometry in Twisted Multilayer Systems, *Nat. Rev. Phys.* **4**, 528–542 (2022).
- [61] J. Wang, J. Cano, A. J. Millis, Z. Liu, and B. Yang, Exact Landau level description of geometry and interaction in a flatband, *Phys. Rev. Lett.* **127**, 246403 (2021).
- [62] J. Wang and Z. Liu, Hierarchy of ideal flatbands in chiral twisted multilayer graphene models, *Phys. Rev. Lett.* **128**, 176403 (2022).
- [13] H. Tian, X. Gao, Y. Zhang, S. Che, T. Xu, P. Cheung, K. Watanabe, T. Taniguchi, M. Randeria, F. Zhang, C. N. Lau, and M. W. Bockrath, Evidence for Dirac flat band superconductivity enabled by quantum geometry, *Nature (London)* **614**, 440 (2023).
- [64] F. D. M. Haldane, Berry curvature on the Fermi surface: Anomalous Hall effect as a topological Fermi-liquid property, *Phys. Rev. Lett.* **93**, 206602 (2004).
- [65] J.-Y. Chen and D. T. Son, Berry Fermi liquid theory, *Annals of Physics* **377**, 345 (2017), arXiv:1604.07857 [cond-mat.str-el].
- [66] Further details of results and calculation are available as supplementary material.
- [67] R. Cheng, Quantum Geometric Tensor (Fubini-Study Metric) in Simple Quantum System: A pedagogical Introduction, arXiv e-prints, arXiv:1012.1337 (2010), arXiv:1012.1337 [quant-ph].
- [68] D. R. Nelson and J. M. Kosterlitz, Universal jump in the superfluid density of two-dimensional superfluids, *Phys. Rev. Lett.* **39**, 1201 (1977).
- [1] A. Altland and B. D. Simons, *Condensed matter field theory* (Cambridge university press, 2010).
- [14] R. Bistritzer and A. H. MacDonald, Moiré bands in twisted double-layer graphene, *Proceedings of the National Academy of Science* **108**, 12233 (2011), arXiv:1009.4203 [cond-mat.mes-hall].
- [71] M. Xie and A. H. MacDonald, Nature of the correlated insulator states in twisted bilayer graphene, *Phys. Rev. Lett.* **124**, 097601 (2020).

## Supplemental Material for ‘‘Ginzburg-Landau theory of flat-band superconductors with quantum metric’’

Shuai A. Chen, K. T. Law

### Appendix A: SM-I: Details on deriving the Free energy

We provide the derivation details of the GL theory, focusing on the isolated flatband system. Our starting point is the Hamiltonian  $H = H_0 + H_{\text{int}}$ , where  $H_0$  represents the free part, and

$$H_{\text{int}} = -g \int d\mathbf{r} a_+^\dagger(\mathbf{r}) a_-^\dagger(\mathbf{r}) a_-(\mathbf{r}) a_+(\mathbf{r}), \quad (\text{A1})$$

represents an attractive interaction. We define the isolated band limit for  $H_0$  as a situation where there exists a large band gap  $W$  between the band around the Fermi energy and the other bands. Moreover, we require that the interaction part does not significantly alter the band structure, which can be expressed as  $W \gg |g|$ . For simplicity, we assume the ideal flatband limit. We can obtain an effective Hamiltonian,

$$H_0 = 0, \quad (\text{A2})$$

in the low-energy limit. To handle the interaction, we introduce the Hubbard-Stratonovich (HS) transformation,

$$1 = \int \mathcal{D}[\Delta, \bar{\Delta}] e^{-g \int_0^\beta d\tau \int d\mathbf{r} [\Delta(\mathbf{r}) - a_-(\mathbf{r}) a_+(\mathbf{r})] [\bar{\Delta}(\mathbf{r}) - \bar{a}_+(\mathbf{r}) \bar{a}_-(\mathbf{r})]}, \quad (\text{A3})$$

where  $\bar{a}, a$  are the Grassmann fields. By employing the HS transformation, we obtain the path integral formulation,

$$Z = \text{Tr} e^{-\beta H_{\text{int}}} = \int \mathcal{D}[\Delta, \bar{\Delta}] e^{-\int_0^\beta d\tau \int d\mathbf{r} |\Delta(\mathbf{r})|^2} \mathcal{Z}[\Delta, \bar{\Delta}], \quad (\text{A4})$$

where

$$\mathcal{Z}[\Delta, \bar{\Delta}] = \int \mathcal{D}[c, \bar{c}] e^{-\int_0^\beta d\tau \int d\mathbf{r} \mathcal{L}[a, \bar{a}, \Delta, \bar{\Delta}]}, \quad (\text{A5})$$

and

$$\mathcal{L}[a, \bar{a}, \Delta, \bar{\Delta}] = (\partial_\tau - \mu)(\bar{a}_+(\mathbf{r}) a_+(\mathbf{r}) + \bar{a}_-(\mathbf{r}) a_-(\mathbf{r})) - g [\Delta(\mathbf{r}) \bar{a}_+(\mathbf{r}) \bar{a}_-(\mathbf{r}) + h.c.]. \quad (\text{A6})$$

As highlighted in the main text, it is crucial to introduce a projection in Eq. (2) in the main text, or alternatively,

$$a_\xi(\mathbf{r}) \rightarrow \frac{1}{N} \sum_{\mathbf{q}} e^{i\mathbf{q}\cdot\mathbf{r}} g_{\mathbf{q}\xi}^*(\alpha) c_{\mathbf{q}\xi}, \quad (\text{A7})$$

to explicitly incorporate the Bloch wave, where  $\alpha$  labels the internal degrees of freedom. Consequently, we obtain a projected Lagrangian density  $\mathcal{L}[c, \bar{c}, \Delta, \bar{\Delta}]$ :

$$\mathcal{L}[a, \bar{a}, \Delta, \bar{\Delta}] \rightarrow \mathcal{L}[c, \bar{c}, \Delta, \bar{\Delta}], \quad (\text{A8})$$

where

$$\mathcal{L}[c, \bar{c}, \Delta, \bar{\Delta}] = (\partial_\tau - \mu)(\bar{c}_{\mathbf{q},+} c_{\mathbf{q},+} + \bar{c}_{\mathbf{q},-} c_{\mathbf{q},-}) - \sum_{\mathbf{k}} g[\Gamma(\mathbf{q}, \mathbf{k}) \Delta(\mathbf{k}) \bar{c}_{\mathbf{q}+\frac{\mathbf{k}}{2},+} \bar{c}_{-\mathbf{q}+\frac{\mathbf{k}}{2},-} + h.c.]. \quad (\text{A9})$$

The presence of the form factor  $g\Gamma(\mathbf{q}, \mathbf{k})$  is crucial in describing the interaction between the bosonic field  $\Delta$  and the fermion field  $c$ . Hence, we obtain the GL theory  $F = F[\Delta, \bar{\Delta}]$  using the formula:

$$Z \equiv \int \mathcal{D}[\Delta, \bar{\Delta}] e^{-\beta F[\Delta, \bar{\Delta}]}, \quad (\text{A10})$$



or equivalently,

$$\begin{aligned} F[\Delta, \bar{\Delta}] &= \sum_{\mathbf{k}} g|\Delta(\mathbf{k})|^2 - T \ln \mathcal{Z}[\Delta, \bar{\Delta}] \\ &= \sum_{\mathbf{k}} g|\Delta(\mathbf{k})|^2 - T \int \mathcal{D}[c, \bar{c}] e^{-\int_0^\beta d\tau \int d\mathbf{r} \mathcal{L}[c, \bar{c}, \Delta, \bar{\Delta}]} \end{aligned} \quad (\text{A11})$$

$$= \sum_{\mathbf{k}} g|\Delta(\mathbf{k})|^2 - T \ln \det G, \quad (\text{A12})$$

where  $G$  is the kernel when we arrange  $\mathcal{L}[c, \bar{c}, \Delta, \bar{\Delta}]$  into a matrix form:

$$\mathcal{L}[c, \bar{c}, \Delta, \bar{\Delta}] = \sum_{\mathbf{q}'\mathbf{q}} \begin{bmatrix} \bar{c}_{\mathbf{q}',+} \\ c_{-\mathbf{q}',-} \end{bmatrix} G_{\mathbf{q}'\mathbf{q}} \begin{bmatrix} c_{\mathbf{q},+} \\ \bar{c}_{-\mathbf{q},-} \end{bmatrix}. \quad (\text{A13})$$

The subsequent step involves expanding the determinant  $\ln \det G$  using standard procedures [1].

Here we alternatively employ the Gor'kov's Green function approach. We first expand the bosonic field  $\Delta(\mathbf{k})$  around the extremum of the free energy as:

$$\Delta(\mathbf{k}) = \Delta_0 \delta_{\mathbf{k},0} + \delta\Delta(\mathbf{k}), \quad (\text{A14})$$

where  $\Delta_0$  represents the mean field solution and  $\delta\Delta(\mathbf{k})$  represents the fluctuations. We assume  $\Delta_0$  to be real with a proper gauge choice. This decomposition splits the Lagrangian  $\mathcal{L}[c, \bar{c}, \Delta, \bar{\Delta}]$  into two parts:

$$\mathcal{L}[c, \bar{c}, \Delta, \bar{\Delta}] = \mathcal{L}_0 + \mathcal{L}_{\text{int}}, \quad (\text{A15})$$

where  $\mathcal{L}_0$  at the leading order reproduces the BCS mean field theory:

$$\mathcal{L}_0 = (\partial_\tau - \mu)(\bar{c}_{\mathbf{q},+} c_{\mathbf{q},+} + \bar{c}_{\mathbf{q},-} c_{\mathbf{q},-}) - g[\Gamma(\mathbf{q}) \Delta_0 \bar{c}_{\mathbf{q},+} \bar{c}_{-\mathbf{q},-} + h.c.], \quad (\text{A16})$$

with

$$\Gamma(\mathbf{q}) \equiv \Gamma(\mathbf{q}, \mathbf{0}) = \sum_{\alpha} g_{-\mathbf{q},+}(\alpha) g_{\mathbf{q},-}(\alpha), \quad (\text{A17})$$

where  $\Gamma(\mathbf{q}) \equiv \Gamma(\mathbf{q}, \mathbf{0}) = \sum_{\alpha} g_{-\mathbf{q},+}(\alpha) g_{\mathbf{q},-}(\alpha)$  represents the interaction term. The interaction Lagrangian  $\mathcal{L}_{\text{int}}$  characterizes the coupling between fluctuations  $\delta\Delta(\mathbf{k})$  and fermions  $c$ ,

$$\mathcal{L}_{\text{int}} = -g \sum_{\mathbf{q}} [\Gamma(\mathbf{q}, \mathbf{k}) \delta\Delta(\mathbf{k}) \bar{c}_{\mathbf{q}+\frac{\mathbf{k}}{2},+} \bar{c}_{-\mathbf{q}+\frac{\mathbf{k}}{2},-} + h.c.]. \quad (\text{A18})$$

Accordingly, we can decompose the free energy  $F[\Delta, \bar{\Delta}]$  in terms of the fluctuations  $\delta\Delta(\mathbf{k})$ ,

$$F[\Delta, \bar{\Delta}] = F_0 + \delta F, \quad (\text{A19})$$

where  $F_0$  represents the mean-field contribution and  $\delta F$  accounts for the fluctuations. The expression for  $F_0$  is given by:

$$F_0 = \sum_{\mathbf{k}} g|\Delta_0|^2 - T \int \mathcal{D}[c, \bar{c}] e^{-\int_0^\beta d\tau \sum_{\mathbf{k}} \mathcal{L}_0}, \quad (\text{A20})$$

$$\begin{aligned} \delta F &= \sum_{\mathbf{k}} g|\delta\Delta|^2 - T \int \mathcal{D}[c, \bar{c}] e^{-\int_0^\beta d\tau \sum_{\mathbf{k}} \mathcal{L}_0} \left( e^{-\int_0^\beta d\tau \sum_{\mathbf{k}} \mathcal{L}_{\text{int}}} - 1 \right) \\ &\equiv \sum_{\mathbf{k}} g|\delta\Delta|^2 - T \left\langle \left( e^{-\int_0^\beta d\tau \sum_{\mathbf{k}} \mathcal{L}_{\text{int}}} - 1 \right) \right\rangle, \end{aligned} \quad (\text{A21})$$

where  $\langle \cdot \rangle$  denotes the thermal average.

The mean-field value  $\Delta_0$  is determined by solving the self-consistent equation  $\frac{\delta F}{\delta \Delta_0} = \frac{\delta F}{\delta \bar{\Delta}_0} = 0$ , which is given by Eq. (6) in

the main text. Once we find the value of  $\Delta_0$ , we can evaluate  $F_0$ , which represents the grand potential, as

$$\begin{aligned} F_0 &= gV|\Delta_0|^2 - T \ln \int \mathcal{D}[c] e^{-\int_0^\beta d\tau \sum_{\mathbf{k}} \mathcal{L}_0} \\ &= gV|\Delta_0|^2 - \sum_{\mathbf{k}} \left[ 2 \ln(1 + e^{-\beta\epsilon(\mathbf{k})}) - \epsilon(\mathbf{k}) \right], \end{aligned} \quad (\text{A22})$$

with  $V$  denoting the system volume.

To evaluate  $\delta F$  and consider fluctuations around the mean field, we can use Gor'kov's normal and abnormal Green functions  $\mathcal{G}(q)$  and  $\mathcal{F}(q)$ , respectively. These functions are defined as

$$\mathcal{G}(q) \equiv \langle c_{\mathbf{q},+}(\omega) \bar{c}_{\mathbf{q},+}(\omega) \rangle = \langle c_{\mathbf{q},-}(\omega) \bar{c}_{\mathbf{q},-}(\omega) \rangle = \frac{i\omega + \mu}{\omega^2 + \epsilon^2(\mathbf{q})}, \quad (\text{A23})$$

$$\mathcal{F}(q) \equiv \langle c_{-\mathbf{q},-}(-\omega) c_{\mathbf{q},+}(\omega) \rangle = \frac{g\Gamma^*(\mathbf{q})\Delta_0}{\omega^2 + \epsilon^2(\mathbf{q})}. \quad (\text{A24})$$

where  $q = (\omega, \mathbf{q})$  represents the frequency and momentum. In orders of  $\delta\Delta$ , we can have perturbative expansion

$$\delta F = F_2 + F_4 + \dots, \quad (\text{A25})$$

where terms up to second order in  $\delta\Delta(\mathbf{k})$  are included. Since the mean field value is stable, there is no linear term in  $\delta\Delta(\mathbf{k})$ . If we neglect temporal fluctuations, we can focus on the second-order term  $F_2$ , which corresponds to Gaussian fluctuations. Evaluating  $F_2$  gives

$$\begin{aligned} F_2 &= \sum_{\mathbf{k}} g |\delta\Delta(\mathbf{k})|^2 - T \frac{1}{2} \left\langle \left( \int_0^\beta d\tau \sum_{\mathbf{k}} \mathcal{L}_{\text{int}} \right)^2 \right\rangle \\ &= \sum_{\mathbf{k}} g |\delta\Delta(\mathbf{k})|^2 - T \sum_{\mathbf{k}} g^2 |\Gamma(\mathbf{q}, \mathbf{k})|^2 |\delta\Delta(\mathbf{k})|^2 \left[ \langle \bar{c}_{\mathbf{q}+\frac{\mathbf{k}}{2},+} \bar{c}_{-\mathbf{q}+\frac{\mathbf{k}}{2},-} \rangle \langle c_{-\mathbf{q}+\frac{\mathbf{k}}{2},-} c_{\mathbf{q}+\frac{\mathbf{k}}{2},+} \rangle \right. \\ &\quad \left. + \frac{1}{2} \langle c_{\mathbf{q}+\frac{\mathbf{k}}{2},+} c_{-\mathbf{q}-\frac{\mathbf{k}}{2},-} \rangle \langle c_{-\mathbf{q}+\frac{\mathbf{k}}{2},-} c_{\mathbf{q}+\frac{\mathbf{k}}{2},+} \rangle + \frac{1}{2} \langle \bar{c}_{\mathbf{q}+\frac{\mathbf{k}}{2},+} \bar{c}_{-\mathbf{q}-\frac{\mathbf{k}}{2},-} \rangle \langle \bar{c}_{-\mathbf{q}+\frac{\mathbf{k}}{2},-} \bar{c}_{\mathbf{q}+\frac{\mathbf{k}}{2},+} \rangle \right] \\ &\equiv \sum_{\mathbf{k}} |\delta\Delta(\mathbf{k})|^2 [g - g^2 \chi(\mathbf{k})]. \end{aligned} \quad (\text{A26})$$

where  $\chi(\mathbf{k})$  takes the form as Eq. (9) in the main text.

## Appendix B: SM-II: Quantum metric and Wannier functions

In the limit of zero temperature, the minimal size of the Cooper pair is solely determined by the quantum metric. This fundamental concept characterizes the geometric properties of the electronic band structure. Remarkably, even with stronger interactions, it is impossible to bind the electrons any closer together. To gain a better understanding, we delve into the explanation of the quantum metric and the optically localized size of Wannier wave functions. Interested readers can also refer to Refs. [2, 3].

We begin with the single-particle Schrödinger equation in  $d$  spatial dimensions

$$H|\psi\rangle = \left[ -\frac{(\hbar\nabla)^2}{2m} + V(\mathbf{r}) \right] |\psi\rangle, \quad (\text{B1})$$

where  $V(\mathbf{r} + \mathbf{a}_i) = V(\mathbf{r})$  represents a periodic potential, and  $\mathbf{a}_i$  ( $i = 1, \dots, d$ ) defines a lattice system. According to the Bloch theorem, the solutions, known as Bloch waves, for an energy band  $n$  can be expressed as:

$$\psi_{n\mathbf{k}}(\mathbf{r}) = e^{i\mathbf{k}\cdot\mathbf{r}} u_{n\mathbf{k}}(\mathbf{r}), \quad (\text{B2})$$

where  $u_{n\mathbf{k}}(\mathbf{r})$  is a periodic Bloch function satisfying  $u_{n\mathbf{k}}(\mathbf{r}) = u_{n\mathbf{k}}(\mathbf{r} + \mathbf{a}_i)$ , and  $\mathbf{k}$  is the Bloch wavevector. The normalization

condition for  $u_{n\mathbf{k}}(\mathbf{r})$  is given by:

$$\int_{\text{u.c.}} d^d \mathbf{r} |u_{n\mathbf{k}}(\mathbf{r})|^2 = 1, \quad (\text{B3})$$

where the integral is taken over one unit cell. Here, u.c. represents the unit cell with volume  $\mathcal{A}_{\text{uc}}$ . The energy  $\epsilon_n(\mathbf{k})$  satisfies periodicity with respect to the reciprocal lattice vectors  $\mathbf{G}_i$ , given by the condition  $\mathbf{a}_i \cdot \mathbf{G}_j = 2\pi\delta_{ij}$ . In other words, the energy is invariant under translations by the reciprocal lattice vectors.

We consider composite bands labeled by the band index  $n$  in a specific subset  $\mathcal{V}$ , which is separated from other bands by sufficiently large band gaps. In this case, we can construct a set of Wannier basis states  $\{|\mathbf{r}_i\alpha\rangle\}$  that span the same sub-Hilbert space as the Bloch waves corresponding to the bands with indices  $n \in \mathcal{V}$ . The Wannier basis states can be expressed as follows:

$$|\mathbf{r}_i\alpha\rangle = \frac{\mathcal{A}_{\text{uc}}}{(2\pi)^d} \int_{\text{BZ}} d^d \mathbf{k} e^{i\mathbf{k}\cdot(\mathbf{r}-\mathbf{r}_i)} \sum_{n \in \mathcal{V}} (\mathcal{U}_{\mathbf{k}})_{n,\alpha} |u_{n\mathbf{k}}\rangle, \quad (\text{B4})$$

$$|u_{n\mathbf{k}}\rangle = \sum_{\mathbf{r}_i} \sum_{\alpha} e^{-i\mathbf{k}\cdot(\mathbf{r}-\mathbf{r}_i)} (\mathcal{U}_{\mathbf{k}}^\dagger)_{\alpha,n} |\mathbf{r}_i\alpha\rangle. \quad (\text{B5})$$

Here,  $\mathcal{A}_{\text{uc}}$  is the volume of the unit cell, and  $\mathbf{r}_i$  represents a lattice site spanned by the lattice vectors  $\mathbf{a}_i$  ( $i = 1, \dots, d$ ). The integration over momentum is performed over the first Brillouin zone (BZ). The unitary matrix  $\mathcal{U}_{\mathbf{k}}$  is chosen to optimize the localization of the Wannier functions. The Wannier function  $\langle \mathbf{r} | \mathbf{r}_i\alpha \rangle \equiv w_\alpha(\mathbf{r} - \mathbf{r}_i)$  is localized around the lattice site  $\mathbf{r}_i$ . It turns out to be the Fourier transformation of the corresponding Bloch wave, and thus inherits the orthonormality properties of the Bloch functions.

The unitary matrix  $\mathcal{U}_{\mathbf{k}}$  is chosen to maximize the localization of Wannier functions by minimizing a localization functional, as introduced by Marzari and Vanderbilt in their seminal work [2]. The localization functional is given by

$$F = \sum_{\alpha \in \mathcal{V}} [\langle \mathbf{0}\alpha | r^2 | \mathbf{0}\alpha \rangle - |\langle \mathbf{0}\alpha | \mathbf{r} | \mathbf{0}\alpha \rangle|^2] = F_I + \delta F. \quad (\text{B6})$$

Both parts,  $F_I$  and  $\delta F$ , are non-negative, where

$$F_I = \sum_{\alpha \in \mathcal{V}} \left[ \langle \mathbf{0}\alpha | r^2 | \mathbf{0}\alpha \rangle - \sum_{\mathbf{r}_i} \sum_{\beta} |\langle \mathbf{r}_i\beta | \mathbf{r} | \mathbf{0}\alpha \rangle|^2 \right], \quad (\text{B7})$$

$$\delta F = \sum_{\mathbf{r}_i (\neq \mathbf{0})} \sum_{\beta (\neq \alpha)} |\langle \mathbf{r}_i\beta | \mathbf{r} | \mathbf{0}\alpha \rangle|^2. \quad (\text{B8})$$

The optimization of the unitary matrix  $\mathcal{U}_{\mathbf{k}}$  aims to minimize the localization functional  $F$ , leading to the construction of maximally localized Wannier functions. The term  $F_I$  is independent of the unitary transformation  $\mathcal{U}_{\mathbf{k}}$  and therefore gauge invariant. This allows us to choose  $\mathcal{U}_{\mathbf{k}}$  as an identity matrix with components  $(\mathcal{U}_{\mathbf{k}})_{\alpha,n} = \delta_{\alpha,n}$  when calculating  $F_I$ . Then from the relation in Eqs. (B4) and (B5), we have

$$\langle u_{n\mathbf{k}} | u_{m\mathbf{k}+\mathbf{q}} \rangle = \sum_{\mathbf{r}_i} e^{-i\mathbf{k}\cdot\mathbf{r}_i} \langle \mathbf{r}_i n | e^{-i\mathbf{q}\cdot\mathbf{r}} | \mathbf{0} m \rangle, \quad (\text{B9})$$

By taking the derivative with respect to  $\mathbf{q}$  on both sides of Eq. (B9), we obtain a series of relations in the limit  $q \rightarrow 0$ . For example, taking the first and second derivatives with respect to  $\mathbf{q}$  gives

$$\langle u_{n\mathbf{k}} | \nabla_{\mathbf{k}} u_{m\mathbf{k}} \rangle = -i \sum_{\mathbf{r}_i} e^{-i\mathbf{k}\cdot\mathbf{r}_i} \langle \mathbf{r}_i n | \mathbf{r} | \mathbf{0} m \rangle, \quad (\text{B10})$$

$$\langle u_{n\mathbf{k}} | \nabla_{\mathbf{k}}^2 u_{m\mathbf{k}} \rangle = - \sum_{\mathbf{r}_i} e^{-i\mathbf{k}\cdot\mathbf{r}_i} \langle \mathbf{r}_i n | \mathbf{r}^2 | \mathbf{0} m \rangle, \quad (\text{B11})$$

Similarly, we can establish the converse relations

$$\langle \mathbf{r}_i n | \mathbf{r} | \mathbf{0} m \rangle = i \frac{\mathcal{A}_{\text{uc}}}{(2\pi)^d} \int_{\text{BZ}} d^d \mathbf{k} e^{i\mathbf{k} \cdot \mathbf{r}_i} \langle u_{n\mathbf{k}} | \nabla_{\mathbf{k}} u_{m\mathbf{k}} \rangle, \quad (\text{B12})$$

$$\langle \mathbf{r}_i n | \mathbf{r}^2 | \mathbf{0} m \rangle = \frac{\mathcal{A}_{\text{uc}}}{(2\pi)^d} \int_{\text{BZ}} d^d \mathbf{k} e^{i\mathbf{k} \cdot \mathbf{r}_i} \langle \nabla_{\mathbf{k}} u_{n\mathbf{k}} | \nabla_{\mathbf{k}} u_{m\mathbf{k}} \rangle. \quad (\text{B13})$$

Therefore, we can simplify  $F_I$  as

$$F_I = \sum_{\alpha \in \mathcal{V}} \left[ \langle \mathbf{0} \alpha | r^2 | \mathbf{0} \alpha \rangle - \sum_{\mathbf{r}_i} \sum_{\beta} |\langle \mathbf{r}_i \beta | \mathbf{r} | \mathbf{0} \alpha \rangle|^2 \right] \quad (\text{B14})$$

$$= \frac{\mathcal{A}_{\text{uc}}}{(2\pi)^d} \int_{\text{BZ}} d^d \mathbf{k} \sum_{n \in \mathcal{V}} \text{Re} \langle \nabla_{\mathbf{k}} u_{n\mathbf{k}} | (\mathbb{I}_{\mathcal{V}} - |u_{n\mathbf{k}}\rangle \langle u_{n\mathbf{k}}|) | \nabla_{\mathbf{k}} u_{n\mathbf{k}} \rangle, \quad (\text{B15})$$

where  $\mathbb{I}_{\mathcal{V}}$  is the identity operator in the sub-Hilbert space spanned by bands carrying indices in  $\mathcal{V}$ . This expression clearly shows that  $F_I$  is expressed in terms of the quantum metric, as defined in Eq. (11) of the main text. Since  $\delta F \geq 0$ , we have the inequality relation,

$$F \geq F_I. \quad (\text{B16})$$

Hence, we can conclude that the quantum metric characterizes an obstruction to finding a complete set of exponentially localized Wannier functions. When  $F_I$  is finite, it indicates that more bands need to be included in the composite bands in order to construct a complete set of exponentially localized Wannier functions.

Another perspective on the quantum metric arises from considering a multiband tight-binding model. Assuming we have already obtained a complete set of exponentially localized Wannier functions constructed from composite bands, we can approximate the continuum Hamiltonian in Eq. (B1) with a tight-binding model. In the language of second quantization, the continuum model in Eq. (B1) can be expressed as

$$H = \int d^d \mathbf{r} \psi^\dagger(\mathbf{r}) \left[ -\frac{(\hbar \nabla)^2}{2m} + V(\mathbf{r}) \right] \psi(\mathbf{r}). \quad (\text{B17})$$

We then expand the field operator  $\psi(\mathbf{r})$  in the basis of Wannier functions

$$\psi(\mathbf{r}) = \sum_{\mathbf{r}_i} \sum_{\alpha \in \mathcal{V}} w_{\alpha}(\mathbf{r} - \mathbf{r}_i) a_{i\alpha} + \sum_{\mathbf{r}_i} \sum_{\beta \in \mathcal{V}^\perp} w_{\beta}^\perp(\mathbf{r} - \mathbf{r}_i) b_{i\beta}, \quad (\text{B18})$$

where  $w_{\beta}^\perp(\mathbf{r} - \mathbf{r}_i)$  denotes Wannier functions associated with the complementary band set  $\mathcal{V}^\perp$ . By substituting the expansion into the Hamiltonian in Eq. (B17), we can derive a tight-binding model defined on the lattice  $\{\mathbf{r}_i\}$

$$\begin{aligned} H &= \sum_{\alpha, \beta \in \mathcal{V}} \sum_{\mathbf{r}_i, \mathbf{r}_j} \langle \mathbf{r}_i \alpha | H | \mathbf{r}_j \beta \rangle a_{i\alpha}^\dagger a_{j\beta} + \sum_{\alpha', \beta' \in \mathcal{V}^\perp} \sum_{\mathbf{r}_i, \mathbf{r}_j} \langle \mathbf{r}_i \alpha' | H | \mathbf{r}_j \beta' \rangle b_{i\alpha'}^\dagger b_{j\beta'} \\ &= \sum_{\alpha, \beta \in \mathcal{V}} \sum_{\mathbf{r}_i, \mathbf{r}_j} t_{ij, \alpha\beta} a_{i\alpha}^\dagger a_{j\beta} + \sum_{\alpha', \beta' \in \mathcal{V}^\perp} \sum_{\mathbf{r}_i, \mathbf{r}_j} t_{ij, \alpha'\beta'}^\perp b_{i\alpha'}^\dagger b_{j\beta'}, \end{aligned} \quad (\text{B19})$$

where no mixing term between indices from  $\mathcal{V}$  and  $\mathcal{V}^\perp$ . Up to this point, all the derivations have been rigorous, and the expression in Eq. (B19) includes all bands. However, since our interest lies solely in the bands belonging to  $\mathcal{V}$ , we can utilize a complete set of exponentially localized Wannier functions to approximate the Hamiltonian in Eq. (B1) with a multi-band tight-binding model  $H_{\text{tb}}$  by disregarding the  $t^\perp$  terms

$$H_{\text{tb}} = \sum_{\alpha, \beta \in \mathcal{V}} \sum_{\mathbf{r}_i, \mathbf{r}_j} t_{ij, \alpha\beta} a_{i\alpha}^\dagger a_{j\beta} = \sum_{\alpha, \beta \in \mathcal{V}} \sum_{\mathbf{k}} h_{\alpha\beta}(\mathbf{k}) a_{\mathbf{k}\alpha}^\dagger a_{\mathbf{k}\beta}, \quad (\text{B20})$$

where  $t_{ij, \alpha\beta}$  exponentially decays with the distance  $|\mathbf{r}_i - \mathbf{r}_j|$ . In Eq. (B20), we have further introduced the Fourier transformation  $a_{\mathbf{k}\alpha}^\dagger = \frac{1}{\sqrt{N}} \sum_{\mathbf{r}_i} a_{i\alpha}^\dagger e^{i\mathbf{k} \cdot \mathbf{r}_i}$ , where  $N$  represents the total number of lattice sites. In our specific setup, where there is a significant

gap between the targeted band and the others, we can project onto the targeted band using the following expressions

$$a_{i\alpha} \rightarrow \frac{1}{\sqrt{N}} \sum_{\mathbf{k}} e^{i\mathbf{k}\cdot\mathbf{r}_i} g_{\mathbf{k}}^*(\alpha) c_{\mathbf{k}}, \quad (\text{B21})$$

or

$$\psi(\mathbf{r}) \rightarrow \frac{1}{\sqrt{N}} \sum_{\mathbf{k}} e^{i\mathbf{k}\cdot\mathbf{r}_i} g_{\mathbf{k}}^*(\alpha) c_{\mathbf{k}}, \quad (\text{B22})$$

where  $g_{\mathbf{k}}$  represents an eigenvector of  $h_{\alpha\beta}(\mathbf{k})$ , and  $c_{\mathbf{k}}$  annihilates an electron in the targeted band. It is important to note that the index  $\alpha$  appearing in both  $a_{i\alpha}$  and  $g_{\mathbf{k}}(\alpha)$  arises from the realization of a multiband tight-binding model, which accounts for the nontrivial quantum metric or Wannier obstruction. This can be inferred from the quantum metric associated with  $g_{\mathbf{k}}$  as described by Eq. (11) in the main text.

## Appendix C: SM-III: Mean field for the Dirac fermions with pseudo magnetic field

### 1. TBG Flatbands and Harper model

The electronic structure of twisted bilayer graphene (TBG) at the magic angle can be described as Dirac fermions experiencing opposite pseudomagnetic fields [4, 5]. The flatbands in TBG can be mapped to the zeroth pseudo Landau level (pLL), which can be effectively simulated using a time-reversal invariant Harper lattice model [3, 6]. This mapping provides analytical convenience for modeling the superconducting phase. In this context, the Hamiltonian for the two-flavor Dirac fermions in two spatial dimensions is given by

$$H_0 = \sum_{\xi} \int d^2\mathbf{r} \Psi_{\xi}^{\dagger}(\mathbf{r}) [(-i\nabla + \mathbf{A}_{\xi}) \cdot \sigma_{\xi}] \Psi_{\xi}(\mathbf{r}), \quad (\text{C1})$$

In Eq. (C1),  $\Psi_{\xi} = [a_{\xi}, b_{\xi}]^T$  is a two-component spinor representing the two sublattices  $a$  and  $b$ ,  $\xi = \pm$  corresponds to the two flavor degrees of freedom, and  $\sigma_{\xi}$  denotes the Pauli matrix  $\sigma_{\xi} = (\xi\sigma_x, \sigma_y)$ . The uniform pseudomagnetic field is represented by the gauge field  $\mathbf{A}_{\xi} = \xi\mathbf{A}$ , and the TBG flatbands are mapped to the induced zeroth pseudo Landau levels (pLL). Without loss of generality, we set  $\Psi_{\xi} \propto [1, 0]$  with the  $a$ -sublattice being occupied, allowing us to obtain the wave functions of the zeroth pLL.

Therefore, we can consider the Harper model with Hamiltonian  $H = -\sum_{\mathbf{r}, \mathbf{r}'} \sum_{\xi} t_{\mathbf{r}, \mathbf{r}'}^{\xi} a_{\xi}^{\dagger}(\mathbf{r}) a_{\xi}(\mathbf{r}')$ , where  $a_{\xi}(\mathbf{r})$  and  $a_{\xi}^{\dagger}(\mathbf{r})$  are the annihilation and creation operators for electrons with flavor  $\xi = \pm$  at lattice site  $\mathbf{r}$ , respectively. The hopping matrix  $t_{\mathbf{r}, \mathbf{r}'}^{\xi}$  describes the hopping processes between nearest-neighbor sites and is given by

$$t_{\mathbf{r}, \mathbf{r}'}^{\xi} = \omega^{\xi r_y} \delta_{\mathbf{r}-\mathbf{e}_x, \mathbf{r}'} + \omega^{-\xi r_y} \delta_{\mathbf{r}+\mathbf{e}_x, \mathbf{r}'} + \delta_{\mathbf{r}-\mathbf{e}_y, \mathbf{r}'} + \delta_{\mathbf{r}+\mathbf{e}_y, \mathbf{r}'}, \quad (\text{C2})$$

where  $\mathbf{e}_x$  and  $\mathbf{e}_y$  are the unit vectors along the  $x$  and  $y$  directions, respectively. The factor  $\omega^{\pm\xi j_y}$  introduces a lattice version of the Landau gauge, and we consider a uniform commensurate flux  $\Phi = \frac{2\pi}{N_o}$ , where  $\omega = e^{i\Phi}$ , such that  $Ba^2 = \frac{2\pi}{N_o}$ , with  $B$  being the pseudomagnetic field. The lattice has  $N_c \times N_o$  sites, with  $N_c$  being the number of super unit cells and  $N_o$  being the number of orbitals. In the reduced Brillouin zone (BZ) with  $q_x \in [-\pi/(aN_o), \pi/(aN_o)]$  and  $q_y \in [-\pi/a, \pi/a]$ , the Bloch functions  $g_{\mathbf{q}, \xi}(\alpha)$  for the zeroth pseudo Landau Level (pLL) can be approximated as

$$g_{\mathbf{q}, \xi}(\alpha) \sim \sum_s e^{-iq_x(\alpha - N_o s)a} \phi_0(\alpha - sN_o - \xi \frac{N_o q_y a}{2\pi}). \quad (\text{C3})$$

where  $\phi_0(r)$  is a Gaussian function and  $(\mathbf{r}_c, \alpha)$  denotes the lattice site  $\mathbf{r}$  with orbital index  $\alpha$ .

### 2. BCS mean field on the continuum model

In the BCS mean-field theory applied to the continuum model  $H_0$  in Eq. (C1), we consider the symmetry gauge with  $\mathbf{A}_{\xi}(\mathbf{r}) = \xi \frac{1}{2} B(y, -x)$ , where  $B$  represents the strength of the pseudomagnetic field. At the zeroth pseudo Landau Level (pLL), all

electrons reside on the A-sublattice, and an attractive interaction can be described by the interaction term

$$H_{\text{int}} = -g \int d^2\mathbf{r} a_+^\dagger(\mathbf{r}) a_-^\dagger(\mathbf{r}) a_-(\mathbf{r}) a_+(\mathbf{r}). \quad (\text{C4})$$

where  $g$  represents the strength of the interaction. To proceed, we make a mean-field ansatz by introducing the order parameter  $\Delta(\mathbf{r})$ , defined as:

$$\Delta(\mathbf{r}) = \langle a_-(\mathbf{r}) a_+(\mathbf{r}) \rangle = \sum_n \phi_{n+}(\mathbf{r}) \phi_{n-}(\mathbf{r}) \langle c_{n-} c_{n+} \rangle, \quad (\text{C5})$$

where  $\phi_{n\xi}(\mathbf{r})$  represents the wave function of an electron with angular momentum  $L_z = \xi n$ . The mean-field ansatz allows for a coordinate-dependent order parameter  $\Delta(\mathbf{r})$ . The time-reversal symmetry invariance guarantees that the localization centers of two electrons in a Cooper pair coincide. The BdG equation takes the form as

$$H_{\text{BdG}} = -g \int d^2\mathbf{r} \Delta(\mathbf{r}) [a_+^\dagger(\mathbf{r}) a_-^\dagger(\mathbf{r}) + a_-(\mathbf{r}) a_+(\mathbf{r})], \quad (\text{C6})$$

where we choose a gauge such that  $\Delta$  is real.

In the large pseudomagnetic field ( $B$ ) limit, we can project electrons onto the zeroth pseudo Landau Levels (pLLs) through a truncated expansion. We express the electron operators  $a_+(\mathbf{r})$  and  $a_-(\mathbf{r})$  in terms of the zeroth pLL wave functions

$$a_+(\mathbf{r}) = \sum_n \phi_{0n+}(\mathbf{r}) c_{n+}, \quad (\text{C7})$$

$$a_-(\mathbf{r}) = \sum_n \phi_{0n-}^*(\mathbf{r}) c_{n-}, \quad (\text{C8})$$

where  $c_{n\xi}^\dagger$  creates an electron with angular momentum  $L_z = \xi n$  at the valley  $\xi$ , and  $\phi_{0n\xi}(\mathbf{r})$  represents the wave function of the electron in the zeroth pLL, characterized by a localization center  $\sqrt{2n}\ell_0$ . The operators  $c_{n\pm}$  are associated with the electrons in the zeroth pLLs. By substituting these expressions into the Hamiltonian, we can reformulate the BdG Hamiltonian as

$$H_{\text{BdG}} = - \sum_n \mu (c_{n+}^\dagger c_{n+} + c_{n-}^\dagger c_{n-}) - \sum_n g \Delta_n (c_{n+}^\dagger c_{n-}^\dagger + c_{n-} c_{n+}), \quad (\text{C9})$$

where  $\mu$  is the chemical potential and  $\Delta_n$  is the pairing potential given by

$$\Delta_n = \int d^2\mathbf{r} \phi_{0n+}(\mathbf{r}) \Delta(\mathbf{r}) \phi_{0n-}^*(\mathbf{r}), \quad n = 0, 1, 2, \dots \quad (\text{C10})$$

We can expect a uniform order parameter for any angular momentum. We can diagonalize the BdG Hamiltonian in Eq. (C9) using the Bogoliubov transformation,

$$c_{m+} = u_m \gamma_{m+} - v_m \gamma_{m-}^\dagger, \quad c_{m-}^\dagger = v_m \gamma_{m+} + u_m \gamma_{m-}^\dagger, \quad (\text{C11})$$

with

$$u_n = \frac{1}{\sqrt{2}} \sqrt{1 - \frac{\mu}{\epsilon_n}}, \quad v_n = \frac{1}{\sqrt{2}} \sqrt{1 + \frac{\mu}{\epsilon_n}}. \quad (\text{C12})$$

The dispersion for the quasiparticles is

$$\epsilon_n = \sqrt{\mu^2 + |g \Delta_n|^2}. \quad (\text{C13})$$

Meanwhile, we can determine the order parameter by the self-consistent gap equation,

$$\Delta(\mathbf{r}) = \sum_{n=0} \phi_{0n+}^*(\mathbf{r}) \phi_{0n-}(\mathbf{r}) u_n v_n \tanh \frac{\beta \epsilon_n}{2}. \quad (\text{C14})$$

Equivalently for  $\Delta_n$ , we have the gap equations as

$$\Delta_m = \sum_n K_{nm} u_n v_n \tanh \frac{\beta \epsilon_n}{2}, \quad (\text{C15})$$

with

$$K_{nm} = \int d^2 \mathbf{r} \phi_{0n+} \phi_{0n-}^* \phi_{0m+} \phi_{0m-}^*. \quad (\text{C16})$$

The chemical potential gets shifted according to the number equation

$$2\nu = \lim_{N \rightarrow \infty} \frac{1}{N} \left( \sum_{m=0}^N \langle c_{m+}^\dagger c_{m+} \rangle + \sum_{m=0}^N \langle c_{m-}^\dagger c_{m-} \rangle \right) = 1 + \frac{\mu}{\epsilon} \tanh \frac{\beta \epsilon}{2}. \quad (\text{C17})$$

Here  $2\nu N = 2\nu BS/2\pi$  is the total numbers of electrons occupying the zeroth pLLs with  $S$  the sample area. By coupling the equations (C14) and (C17), we can obtain the pairing order parameter and renormalized chemical potential.

The simplified self-consistent equation for the mean field  $\Delta(\mathbf{r})$  at zero temperature ( $T = 0$ ) allows for an analytical solution. Due to the translational symmetry, the order parameter is constant throughout the system,  $\Delta(\mathbf{r}) \equiv \Delta_0(T = 0)$ . This yields an analytical expression for the mean field at  $T = 0$ , given by

$$\Delta_0(T = 0) = \frac{\sqrt{\nu(1-\nu)}}{2\pi \ell_0^2}, \quad (\text{C18})$$

where  $\nu$  is the filling factor and  $\ell_0$  is the magnetic length. In general cases, numerical methods are required to solve the self-consistent gap equation and find the mean field  $\Delta(\mathbf{r})$  or  $\Delta_n$ . The critical temperature  $T_{\text{MF}}$  and its relation to the magnetic field  $B_r$  are of interest. Near  $T_{\text{MF}}$ , the gap equations can be linearized, resulting in an eigenvalue problem for the matrix  $K_{nm}$ :

$$\Delta_m = \frac{g\bar{\nu}\beta}{4} \sum_n K_{nm} \Delta_n, \quad (\text{C19})$$

where  $\bar{\nu} = \frac{2(1-2\nu)}{\ln(\nu^{-1}-1)}$  and  $\beta$  is the inverse temperature. The critical temperature  $T_{\text{MF}}$  is determined by the condition that the maximal eigenvalue of  $K_{nm}$  satisfies the linearized gap equation. The matrix  $K_{nm}$  has an eigenvector  $\Delta_n = 1$  (for  $n = 0, 1, 2, \dots$ ) with the eigenvalue  $\frac{\ell_0^2}{2}$ , which is the dominant eigenvalue according to the Perron-Frobenius theorem. From this analysis, we identify the critical temperature  $T_{\text{BCS}}$  that is linearly dependent on the magnetic field  $B$

$$T_{\text{MF}} = \bar{\nu} \tau_c, \quad (\text{C20})$$

where  $\tau_c = \frac{g}{8\pi \ell_0^2}$  is the critical temperature and  $\nu = \frac{1}{2}$ . Remarkably, the maximum  $T_{\text{MF}}$  for superconductivity occurs at half-filling, i.e.,  $\mu = 0$ ,  $\nu = 1/2$ . In this case, the quasiparticle spectrum remains flat. However, it is worth noting that a dispersive quasiparticle band can appear when an external magnetic field is applied. Additionally, the characteristic quantity  $g\Delta_0(T = 0)/T_{\text{MF}} = 4\bar{\nu}^{-1} \sqrt{\nu(1-\nu)}$ , and around half-filling  $\nu = 1/2$ ,  $g\Delta_0(T = 0)/T_{\text{MF}} = 2$ . This value is larger than that of a conventional BCS superconductor with a large Fermi velocity.

### 3. The mean field and BKT transition

In the effective theory for the Goldstone mode, we consider a mean-field value  $\Delta_0(T)$  at temperature  $T$  that satisfies the self-consistent equations given in Eq. (C14) or Eq. (6) in the main text. For an isotropic system with a flat quasiparticle band, we collect the self-consistent equations necessary to determine the BKT transition temperature

$$\epsilon = 2\tau_c \tanh \frac{\beta_{\text{BKT}} \epsilon}{2}, \quad (\text{C21})$$

$$2\nu = 1 + \frac{\mu}{\epsilon} \tanh \frac{\beta_{\text{BKT}} \epsilon}{2}, \quad (\text{C22})$$

$$T_{\text{BKT}} = \frac{\pi}{8} g \Delta_0(T_{\text{BKT}}) \frac{\sqrt{\det \bar{\gamma}_2^{ab}}}{\mathcal{A}_{\text{uc}}} \quad (\text{C23})$$

where  $\beta_{\text{BKT}} = T_{\text{BKT}}^{-1}$  and  $\epsilon = \sqrt{|\Delta_0(T_{\text{BKT}})|^2 + \mu^2}$ . The quantum metric  $\sqrt{\det\bar{\gamma}_2^{ab}}$  appears in the expression for the BKT transition temperature. In general, these equations need to be solved numerically. However, when the quantum metric  $\sqrt{\det\bar{\gamma}_2^{ab}}$  is small, such that  $T_{\text{BKT}}$  is much smaller than  $T_{\text{MF}}$ , we can approximate  $\Delta_0(T_{\text{BKT}})$  with the pairing gap e.g.  $\Delta_0$  at  $T = 0$  to approximate  $\Delta_0(T_{\text{BKT}})$ . In this case, a good approximation for the BKT transition temperature is given by

$$T_{\text{BKT}} = \frac{T_{\text{MF}}}{2} \frac{\sqrt{\det\bar{\gamma}_2^{ab}}}{\mathcal{A}_{\text{uc}}}, \quad \text{for small } \sqrt{\det\bar{\gamma}_2^{ab}}. \quad (\text{C24})$$

It is important to note that the quantum metric  $\sqrt{\det\bar{\gamma}_2^{ab}}$  possesses its own independent degree of freedom and can be tuned to be sufficiently large. As a result, the BKT transition temperature can become comparable to  $T_{\text{MF}}$ . To further illustrate this point, we can linearize the self-consistent equations at half-filling ( $\mu = 0$ ) for simplicity. Using the expansion  $\tanh x = x - \frac{1}{3}x^3 + \mathcal{O}(x^5)$ , we obtain the equation

$$g\Delta_0(T_{\text{BKT}}) = 2\tau_0 \left[ \frac{\beta_{\text{BKT}}g\Delta_0(T_{\text{BKT}})}{2} - \frac{1}{3} \left( \frac{\beta_{\text{BKT}}g\Delta_0(T_{\text{BKT}})}{2} \right)^3 \right], \quad (\text{C25})$$

$$T_{\text{BKT}} = \frac{\pi}{8} g\Delta_0(T_{\text{BKT}}) \frac{\sqrt{\det\bar{\gamma}_2^{ab}}}{\mathcal{A}_{\text{uc}}}. \quad (\text{C26})$$

and one can solve them with a solution

$$T_{\text{BKT}} = \frac{12\alpha^2 - 1}{12\alpha^2} T_{\text{MF}}, \quad \Delta_0(T_{\text{BKT}}) = \frac{12\alpha^2 - 1}{12\alpha^3} T_{\text{MF}}, \quad (\text{C27})$$

with  $\alpha \equiv \frac{\pi}{8} \frac{\sqrt{\det\bar{\gamma}_2^{ab}}}{\mathcal{A}_{\text{uc}}}$ . It is evident that in the limit  $\alpha \rightarrow \infty$ , the BKT transition temperature  $T_{\text{BKT}}$  approaches the mean-field transition temperature  $T_{\text{MF}}$

$$T_{\text{BKT}} \rightarrow T_{\text{MF}}, \quad \text{for large } \sqrt{\det\bar{\gamma}_2^{ab}} \quad (\text{C28})$$

This observation holds true for arbitrary fillings as well.

#### Appendix D: SM-IV: Harper model and the effective GL theory

We can employ a time-reversal invariant (TRI) Harper lattice model to regularize the zeroth Landau level (pLL) in a system with  $N = N_c \times N_o$  lattice sites, where  $N_c$  is the number of super unit cells and  $N_o$  is the number of orbitals per super unit cell.

We can regularize the zeroth pLL using a TRI Harper lattice model on a system  $N = N_c \times N_o$  with  $N_c$  super unit cells and  $N_o$  orbitals. To facilitate this regularization, we relabel the original lattice site as  $\mathbf{r} = (\mathbf{r}_c, \alpha)$ , where  $\mathbf{r}_c$  represents the super unit cell and  $\alpha$  denotes the orbital index. By introducing multi-band fermion operators  $a_\xi(\mathbf{r}_c, \alpha)$ , which annihilate fermions at the specified super unit cell  $\mathbf{r}_c$  and orbital  $\alpha$ , we can effectively describe the fermionic degrees of freedom on the TRI Harper lattice. In this framework, we can reformulate the attractive interaction given in Eq. (1) of the main text as

$$H_{\text{int}} = -g \sum_{\mathbf{r}_c, \alpha} a_+^\dagger(\mathbf{r}_c, \alpha) a_-^\dagger(\mathbf{r}_c, \alpha) a_-(\mathbf{r}_c, \alpha) a_+(\mathbf{r}_c, \alpha). \quad (\text{D1})$$

In this context, the auxiliary field  $\Delta_\alpha(\mathbf{r}_c)$  now acquires a dependence on the orbital index, given by

$$\Delta_\alpha(\mathbf{r}_c) = a_-(\mathbf{r}_c, \alpha) a_+(\mathbf{r}_c, \alpha). \quad (\text{D2})$$

By applying the Hubbard-Stratonovich transformation, we can express the interaction part of the Lagrangian within the path integral framework

$$\begin{aligned} L_{\text{int}}[a, \bar{a}, \Delta, \bar{\Delta}] &= - \sum_{\mathbf{r}_c, \alpha} g [\Delta_\alpha(\mathbf{r}_c) \bar{a}_+(\mathbf{r}_c, \alpha) \bar{a}_-(\mathbf{r}_c, \alpha) + \text{h.c.}] \\ &= - \sum_{\mathbf{k}, \mathbf{q}, \alpha} g \left[ \Gamma_\alpha(\mathbf{q}, \mathbf{k}) \Delta_\alpha(\mathbf{k}) \bar{c}_{\mathbf{k}+\frac{\mathbf{q}}{2}, +} \bar{c}_{-\mathbf{k}+\frac{\mathbf{q}}{2}, -} + \text{h.c.} \right]. \end{aligned} \quad (\text{D3})$$



In the second line, we perform a projection onto the zeroth pLL

$$a_\xi(\mathbf{r}_c, \alpha) \rightarrow \sum_{\mathbf{k}} e^{-i\mathbf{k}\cdot\mathbf{r}_c} g_{\mathbf{k},\xi}^*(\alpha) c_{\mathbf{k}\xi}, \quad (\text{D4})$$

where

$$\Gamma_\alpha(\mathbf{q}, \mathbf{k}) = g_{\mathbf{k}+\frac{\mathbf{q}}{2},+}(\alpha) g_{-\mathbf{k}+\frac{\mathbf{q}}{2},-}(\alpha). \quad (\text{D5})$$

The Bloch wave  $g_{\mathbf{k},\xi}(\alpha)$  captures the orbital dependence, and the normalization condition  $\frac{1}{N_c} \sum_{\mathbf{k}} |g_{\mathbf{k}}(\alpha)|^2 = \frac{1}{N_{\text{orb}}}$  is satisfied, taking into account the enlargement of the unit cell. Combining the interaction Lagrangian  $L_{\text{int}}$  with the free fermion part  $L_0 = \sum_{\mathbf{k}\xi} (-i\omega - \mu) \bar{c}_{\mathbf{k}\xi} c_{\mathbf{k}\xi}$ , we obtain the total Lagrangian  $L = L_0 + L_{\text{int}}$ .

We can expand the bosonic field around the mean field configuration:

$$\Delta_\alpha(\mathbf{k}) = \Delta_{\alpha 0} \delta_{\mathbf{k}0} + \delta\Delta_\alpha(\mathbf{k}), \quad (\text{D6})$$

which decomposes the Lagrangian  $L$  into two parts. The first part corresponds to the BCS mean field and can be expressed as:

$$\mathcal{L}_0[c, \bar{c}] = (-i\omega - \mu) (\bar{c}_{\mathbf{q},+} c_{\mathbf{q},+} + \bar{c}_{\mathbf{q},-} c_{\mathbf{q},-}) - \sum_{\alpha} [\Gamma_\alpha(\mathbf{q}) \Delta_\alpha \bar{c}_{\mathbf{q},+} \bar{c}_{-\mathbf{q},-} + \text{h.c.}], \quad (\text{D7})$$

where  $\Gamma_\alpha(\mathbf{q}) \equiv \Gamma_\alpha(\mathbf{q}, 0)$ . From this, we can derive the Bogoliubov quasiparticle dispersion relation  $\epsilon(\mathbf{q}) = \sqrt{|g \sum_{\alpha} \Gamma_\alpha(\mathbf{q}) \Delta_{\alpha 0}|^2 + \mu^2}$  as well as the self-consistent equation for  $\Delta_{\alpha 0}$  given by:

$$\Delta_{\alpha 0} = \frac{1}{N_c} \sum_{\mathbf{q}} \sum_{\gamma} \Delta_{\gamma 0} \frac{\Gamma_\alpha(\mathbf{q}) \Gamma_\gamma^*(\mathbf{q})}{2\epsilon_{\mathbf{q}}} \tanh \frac{\beta\epsilon_{\mathbf{q}}}{2}. \quad (\text{D8})$$

We can neglect the fluctuations in the orbital indices and make the approximation:

$$\Delta_\alpha(\mathbf{k}) \equiv \Delta(\mathbf{k}), \quad \Delta_{\alpha 0} \equiv \Delta_0 \quad \forall \alpha, \quad (\text{D9})$$

which simplifies the calculations while capturing the main physics. By integrating out the fermion fields and considering the phase fluctuations  $\delta\Delta(\mathbf{r}) = \Delta_0 e^{2i\theta(\mathbf{r})} - \Delta_0 \simeq 2i\theta(\mathbf{r})\Delta_0$  (ignoring amplitude fluctuations), we obtain the effective action for the phase fluctuations:

$$\mathcal{L}[\theta] = \frac{1}{2} D_s (\nabla\theta)^2, \quad (\text{D10})$$

where  $D_s$  is called superfluid weight that characterizes the stiffness of the phase fluctuations. For the zeroth pLL, the factors are given by  $\gamma_0(\mathbf{q}) = 1$  and  $\gamma_2^{ab}(\mathbf{q}) = \frac{N_o a^2}{4\pi} \delta_{ab}$  [3, 12]. At temperature  $T = 0$ , according to Eq. (13) in the main text, the superfluid weight is defined as  $D_s \equiv \frac{(g\Delta_0)^2}{2\pi\epsilon}$ . For filling around  $\mu = 0$ , the ratio  $D_s/(g\Delta_0) \sim 0.16$ , which is in good agreement with experimental results [13].

### Appendix E: SM-V: Model for twisted bilayer graphene

For the twisted bilayer graphene (TBG) system [14], we consider the AA-stacking configuration where the two layers  $\ell = 1$  and  $\ell = 2$  are rotated around a pair of registered B sites by angles  $-\theta/2$  and  $+\theta/2$ , respectively. Before rotation, the lattice vectors are denoted as  $\mathbf{a}_1 = a(1, 0)$  and  $\mathbf{a}_2 = a(1/2, \sqrt{3}/2)$  for the AA-stacked bilayer, where  $a = 0.246$  nm is the lattice constant of graphene. The corresponding reciprocal lattice vectors are  $\mathbf{g}_1 = \frac{2\pi}{a}(1, -1/\sqrt{3})$  and  $\mathbf{g}_2 = \frac{2\pi}{a}(0, 2/\sqrt{3})$ . After rotation, the lattice vectors  $\mathbf{a}^{(\ell)}$  of the two layers  $\ell = 1, 2$  can be constructed as  $\mathbf{a}_i^{(1)} = R(-\theta/2)\mathbf{a}_i$  and  $\mathbf{a}_i^{(2)} = R(+\theta/2)\mathbf{a}_i$ , where  $R(\theta)$  is the rotation matrix with an angle  $\theta$ . Similarly, the reciprocal lattice vectors for the two layers after rotation are given by  $\mathbf{g}_i^{(1)} = R(-\theta/2)\mathbf{g}_i$  and  $\mathbf{g}_i^{(2)} = R(+\theta/2)\mathbf{g}_i$ . When the rotation angle  $\theta$  is small, the TBG exhibits a moiré pattern with a very long period. The reciprocal lattice vectors for the moiré pattern are given by

$$\mathbf{G}_i^m = \mathbf{g}_i^{(1)} - \mathbf{g}_i^{(2)}. \quad (\text{E1})$$

The real-space lattice vectors  $\mathbf{L}_j^m$  satisfy the condition  $\mathbf{G}_i^m \cdot \mathbf{L}_j^m = 2\pi\delta_{ij}$ , and the moiré lattice constant  $L_m$  is given by  $L_m = |\mathbf{L}_1^m| = |\mathbf{L}_2^m| = \frac{a}{2\sin(\theta/2)}$ .

At small angles, such as  $\theta = 1.08^\circ$  as considered in the main text, an effective continuum model can be applied. In this regime, intervalley mixing can be neglected, allowing for the block-diagonalization of the Hamiltonian. For a given valley  $\rho$  and spin  $\sigma$ , the effective Hamiltonian  $H^{(\rho)}$  takes the form

$$H^{(\sigma\rho)} = H_{\text{kin}}^1 + H_{\text{kin}}^2 + H_{\text{kin}}^\perp - \mu N + H_{\text{int}}. \quad (\text{E2})$$

The first two terms,  $H_{\text{kin}}^\ell$  ( $\ell = 1, 2$ ), describe the intralayer hopping and can be approximated by the two-dimensional Weyl equation

$$\begin{aligned} H_{\text{kin}}^\ell &= - \int d^2\mathbf{r} v_F \psi_{\sigma\rho,\ell}^\dagger(\mathbf{r}) \left[ R(\mp\theta/2)(-i\nabla - \mathbf{K}_\rho^{(\ell)}) \right] \cdot \boldsymbol{\sigma}^\rho \psi_{\sigma\rho,\ell}(\mathbf{r}) \\ &= - \int_{\text{mBZ}} \frac{d^2\mathbf{k}}{(2\pi)^2} v_F \psi_{\sigma\rho,\ell}^\dagger(\mathbf{k}) \left[ R(\mp\theta/2)(\mathbf{k} - \mathbf{K}_\rho^{(\ell)}) \right] \cdot \boldsymbol{\sigma}^\rho \psi_{\sigma\rho,\ell}(\mathbf{k}). \end{aligned} \quad (\text{E3})$$

where  $\mathbf{K}_\rho^{(\ell)} = -\rho[2\mathbf{g}1^{(\ell)} + \mathbf{g}2^{(\ell)}]/3$  for layer  $\ell$  and valley  $\rho$ , and  $(\mp)$  corresponds to  $\rho = 1(2)$  in  $R(\mp\theta/2)$ . Here, mBZ denotes the Brillouin zone for the moiré lattice, and the Fermi velocity is  $v_F = 7.98 \times 10^5$  m/s. The vector  $\psi_{\sigma\rho,\ell}(\mathbf{r})$  represents a sublattice space vector, given by  $\psi_{\sigma\rho,\ell}(\mathbf{r}) = [\psi_{\sigma\rho,\ell A}(\mathbf{r}) \ \psi_{\sigma\rho,\ell B}(\mathbf{r})]^T$ , and the fermion operator  $\psi_{\sigma\rho,\ell\xi}(\mathbf{r})$  annihilates an electron with spin index  $\sigma$ , layer  $\ell$ , and sublattice  $\xi$  at the valley  $\rho$ . The vector  $\boldsymbol{\sigma}^\rho = (\rho\sigma_x, \rho\sigma_y)$  contains the Pauli matrices in the sublattice system ( $\rho = \pm$ ). The third part  $H_{\text{kin}}^\perp$  describes the effective interlayer hopping. It can be written as

$$H_{\text{kin}}^\perp = \int d^2\mathbf{r} \left[ \psi_{\sigma\rho,1A}^\dagger(\mathbf{r}) \ \psi_{\sigma\rho,1B}^\dagger(\mathbf{r}) \right] T_{12}(\mathbf{r}) \begin{bmatrix} \psi_{\sigma\rho,2A}(\mathbf{r}) \\ \psi_{\sigma\rho,2B}(\mathbf{r}) \end{bmatrix} + h.c. \quad (\text{E4})$$

$$= \int d^2\mathbf{r} \sum_{\ell,\xi\xi'} \psi_{\sigma\rho,\ell\xi}^\dagger(\mathbf{r}) T_{\ell\bar{\ell},\xi\xi'}(\mathbf{r}) \psi_{\sigma\rho,\bar{\ell}\xi'}(\mathbf{r}), \quad (\text{E5})$$

where  $\bar{\ell}$  denotes the opposite layer to  $\ell$ . The elements of the  $2 \times 2$  matrix  $[T_{12}(\mathbf{r})]_{\xi\xi'} = T_{12,\xi\xi'}(\mathbf{r})$  have the following form

$$T_{12}(\mathbf{r}) = \begin{bmatrix} t_{AA} & t_{AB} \\ t_{BA} & t_{BB} \end{bmatrix} + \begin{bmatrix} t_{AA} & t_{AB}\omega^{-\xi} \\ t_{BA}\omega^\xi & t_{BB} \end{bmatrix} e^{i\xi\mathbf{G}_1^m \cdot \mathbf{r}} + \begin{bmatrix} t_{AA} & t_{AB}\omega^\xi \\ t_{BA}\omega^{-\xi} & t_{BB} \end{bmatrix} e^{i\xi(\mathbf{G}_1^m + \mathbf{G}_2^m) \cdot \mathbf{r}}. \quad (\text{E6})$$

where  $\omega = e^{2\pi i/3}$ . The TBG system exhibits a corrugation effect, causing variations in the interlayer spacing. Consequently, the model parameters deviate from the condition of a flat TBG, where  $t_{AA} = t_{AB} = t_{BA} = t_{BB}$ . In the optimized lattice structure of TBG, the corrugation occurs in the out-of-plane direction, enabling the use of different parameter values:  $t_{AA} = t_{BB} = 79.7$  meV and  $t_{AB} = t_{BA} = 97.5$  meV, within the effective model. This discrepancy between  $t_{AA}(t_{BB})$  and  $t_{AB}(t_{BA})$  introduces an energy gap between the lowest bands and excited bands, which is consistent with experimental observations [15]. The third term in Eq. (E2) corresponds to the chemical potential, denoted as

$$-\mu N = -\mu \int d^2\mathbf{r} \sum_{\sigma\rho\ell\xi} \psi_{\sigma\rho,\ell\xi}^\dagger(\mathbf{r}) \psi_{\sigma\rho,\ell\xi}(\mathbf{r}), \quad (\text{E7})$$

where  $N$  represents the total number operator, and  $\mu$  is the chemical potential that controls the filling condition of the system. The last term in the equation represents an attractive interaction as previously studied in [16, 17]

$$H_{\text{int}} = -g \int d^2\mathbf{r} \sum_{\sigma_1\sigma_2\rho\ell\xi} \psi_{\sigma_1\rho,\ell\xi}^\dagger(\mathbf{r}) \psi_{\sigma_2\rho,\ell\xi}^\dagger(\mathbf{r}) \psi_{\sigma_2\rho,\ell\xi}(\mathbf{r}) \psi_{\sigma_1\rho,\ell\xi}(\mathbf{r}), \quad (\text{E8})$$

where  $g$  represents the effective attractive interaction potential. The operators  $\psi_{\sigma_1\rho,\ell\xi}(\mathbf{r})$  and  $\psi_{\sigma_2\rho,\ell\xi}(\mathbf{r})$  annihilate electrons with spin indices  $\sigma_1$  and  $\sigma_2$ , respectively, within the same layer  $\ell$ , sublattice  $\xi$ , and valley  $\rho$ .

The mean field theory with an order parameter  $\Delta_{\rho,\ell\xi}(\mathbf{r}) = \langle \psi_{\downarrow\rho,\ell\xi}(\mathbf{r}) \psi_{\uparrow\rho,\ell\xi}(\mathbf{r}) \rangle$  has been extensively investigated in Refs. [16, 17]. However, our current focus is on the critical region. In particular, we are interested in the energy level depicted in Fig. 1(a), which exhibits two nearly flat bands associated with a specific valley  $\rho$  and spin  $\sigma$ . To study these flat bands, we introduce a

projection onto these states, labeled as  $n = 1, 2$ . This projection is achieved by transforming the electron field operator:

$$\psi_{\sigma\rho,\ell\xi}(\mathbf{r}) \rightarrow \int_{\text{mBZ}} \frac{d^2\mathbf{k}}{(2\pi)^2} e^{-i\mathbf{k}\cdot\mathbf{r}} \sum_{n=1,2} g_{\sigma\rho,n\mathbf{k}}^*(\alpha) c_{\sigma\rho,n}(\mathbf{k}), \quad (\text{E9})$$

where  $c_{\sigma\rho,n}(\mathbf{k})$  is the annihilation operator for the  $n$ th band with energy  $h_{\rho,n}(\mathbf{k})$ , and  $\alpha$  represents an additional internal degree of freedom beyond spin and valley. It is worth noting that the unit cell area of the twisted lattice, denoted as  $\mathcal{A}_{\text{uc}}$ , is included in this transformation. By employing this projection, we can focus specifically on the physics associated with the nearly flat bands of interest.

In accordance with the GL theory framework discussed in the main text, we introduce the bosonic auxiliary field  $\Delta_{\rho,\ell\xi}(\mathbf{r}) = \psi_{\downarrow\bar{\rho},\ell\xi}(\mathbf{r})\psi_{\uparrow\rho,\ell\xi}(\mathbf{r})$  and make the approximation of neglecting fluctuations in the layer  $\ell$  and sublattice  $\xi$  by assuming  $\Delta_{\rho,\ell\xi}(\mathbf{r}) = \Delta_{\rho}(\mathbf{r})$ . For notation clarifications, in the critical region where the mean field values vanish, we continue to use  $\Delta_{\rho,\ell\xi}(\mathbf{r})$  to denote the fluctuations. By employing the Hubbard-Stratonovich transformation, we obtain the action for  $\psi_{\sigma\rho,\ell\xi}(\mathbf{r})$  as,

$$Z = \int \mathcal{D}[\Delta, \bar{\Delta}] e^{-g \int_0^\beta d\tau \int d^2\mathbf{r} \sum_{\rho\ell\xi} |\Delta_{\rho,\ell\xi}|^2} \mathcal{Z}[\Delta, \bar{\Delta}], \quad (\text{E10})$$

with

$$\mathcal{Z}[\Delta, \bar{\Delta}] = \int \mathcal{D}[\psi, \bar{\psi}] e^{-\int_0^\beta d\tau \int d^2\mathbf{r} \mathcal{L}[\psi, \bar{\psi}, \Delta, \bar{\Delta}]}, \quad (\text{E11})$$

$$\mathcal{L}[\psi, \bar{\psi}, \Delta, \bar{\Delta}] = \sum_{\sigma\rho\ell\xi} \bar{\psi}_{\sigma\rho,\ell\xi}(\mathbf{r}) [\partial_\tau + h(-i\nabla) - \mu] \psi_{\sigma\rho,\ell\xi}(\mathbf{r}) - g \sum_{\rho\ell\xi} [\bar{\Delta}_{\rho}(\mathbf{r}) \psi_{\downarrow\bar{\rho},\ell\xi}(\mathbf{r}) \psi_{\uparrow\rho,\ell\xi}(\mathbf{r}) + h.c.], \quad (\text{E12})$$

Here,  $h(-i\nabla)$  represents the kinetic operator. After projecting onto the two nearly flat bands, as previously emphasized, it is necessary to incorporate the nontrivial Bloch waves. This entails modifying the Lagrangian

$$\mathcal{L}[\psi, \bar{\psi}, \Delta, \bar{\Delta}] \rightarrow \mathcal{L}[c, \bar{c}, \Delta, \bar{\Delta}]. \quad (\text{E13})$$

The projected Lagrangian  $\mathcal{L}[c, \bar{c}, \Delta, \bar{\Delta}]$  is

$$\mathcal{L}[c, \bar{c}, \Delta, \bar{\Delta}] = \mathcal{L}_0[c, \bar{c}] + \mathcal{L}_{\text{int}}[c, \bar{c}, \Delta, \bar{\Delta}],$$

with the free part for the projected fermions  $c$ ,

$$\mathcal{L}_0[c, \bar{c}] = \sum_{\sigma\rho} \bar{c}_{\sigma\rho,n}(\mathbf{k}) [\partial_\tau + \mathcal{E}_{\rho,n}(\mathbf{k})] c_{\sigma\rho,n}(\mathbf{k}), \quad (\text{E14})$$

and the interaction between bosonic field  $\Delta$  and projected fermions  $c$ ,

$$\mathcal{L}_{\text{int}}[c, \bar{c}, \Delta, \bar{\Delta}] = -\frac{g}{\mathcal{A}_{\text{uc}}} \sum_{\rho} \sum_{n,m} \left[ \Gamma_{\rho,nm}(\mathbf{q}, \mathbf{k}) \bar{\Delta}_{\rho}(\mathbf{k}) c_{\downarrow\bar{\rho},n}(-\mathbf{q} + \frac{\mathbf{k}}{2}) c_{\uparrow\rho,m}(\mathbf{q} + \frac{\mathbf{k}}{2}) + h.c. \right], \quad (\text{E15})$$

where  $\mathcal{E}_{\rho,n}(\mathbf{k}) = h_{\rho,n}(\mathbf{k}) - \mu$ ,  $h_{\rho,n}(\mathbf{k})$  is the dispersion of the targeted band  $n$  and the prefactor  $\Gamma_{\rho,nm}$  is

$$\Gamma_{\rho,nm}(\mathbf{q}, \mathbf{k}) = \sum_{\alpha} g_{\downarrow\rho,n-\mathbf{q}+\frac{\mathbf{k}}{2}}(\alpha) g_{\uparrow\rho,n\mathbf{q}+\frac{\mathbf{k}}{2}}(\alpha). \quad (\text{E16})$$

Around the critical region, we have the Gor'kov's Green function

$$\mathcal{G}_{\rho,n}(q) = \langle c_{\sigma\rho,n}(\mathbf{q}) \bar{c}_{\sigma\rho,n}(\mathbf{q}) \rangle = \frac{1}{-i\omega + \mathcal{E}_{\rho,n}(\mathbf{k})}, \quad (\text{E17})$$

$$\mathcal{F}_{\rho,n}(q) = \langle c_{\sigma\rho,n}(\mathbf{q}) c_{\sigma\rho,n}(-\mathbf{q}) \rangle = 0. \quad (\text{E18})$$

with  $q = (\mathbf{q}, \omega)$ . Integrate out the fermion field and we then have

$$\begin{aligned} F[\Delta, \bar{\Delta}] &= \sum_{\rho} g |\Delta_{\rho}|^2 - \frac{1}{2} \left\langle \left( \int_0^{\beta} d\tau \int \frac{d^2 \mathbf{k}}{(2\pi)^2} \mathcal{L}_{\text{int}}[c, \bar{c}, \Delta, \bar{\Delta}] \right)^2 \right\rangle \\ &= \sum_{\rho} (g - g^2 \chi_{\rho}(\mathbf{k})) |\Delta_{\rho}(\mathbf{k})|^2, \end{aligned} \quad (\text{E19})$$

with

$$\chi_{\rho}(\mathbf{k}) = \frac{T}{2\pi} \sum_{\omega} \int \frac{d^2 \mathbf{q}}{(2\pi)^2} |\Gamma_{\rho, nm}(\mathbf{q}, \mathbf{k})|^2 \mathcal{G}_{\rho, n}(q) \mathcal{G}_{\rho, m}(-q) \quad (\text{E20})$$

$$= \frac{T}{2\pi} \sum_{n, m} \sum_{\omega} \int \frac{d^2 \mathbf{q}}{(2\pi)^2} |\Gamma_{\rho, nm}(\mathbf{q}, \mathbf{k})|^2 \cdot \frac{1}{-i\omega + \mathcal{E}_{\rho, n}(\mathbf{q} + \frac{\mathbf{k}}{2})} \frac{1}{i\omega + \mathcal{E}_{\rho, m}(-\mathbf{q} + \frac{\mathbf{k}}{2})} \quad (\text{E21})$$

$$= \frac{1}{2\pi} \sum_{n, m} \int \frac{d^2 \mathbf{q}}{(2\pi)^2} |\Gamma_{\rho, nm}(\mathbf{q}, \mathbf{k})|^2 \cdot \frac{\tanh\left(\frac{\beta}{2} \mathcal{E}_{\rho, n}(\mathbf{q} + \frac{\mathbf{k}}{2})\right) + \tanh\left(\frac{\beta}{2} \mathcal{E}_{\rho, m}(\mathbf{q} - \frac{\mathbf{k}}{2})\right)}{2(\mathcal{E}_{\rho, n}(\mathbf{q} + \frac{\mathbf{k}}{2}) + \mathcal{E}_{\rho, m}(\mathbf{q} - \frac{\mathbf{k}}{2}))}, \quad (\text{E22})$$

where we use  $\mathcal{E}_{\rho, n}(\mathbf{q} - \frac{\mathbf{k}}{2}) = \mathcal{E}_{\rho, n}(-\mathbf{q} + \frac{\mathbf{k}}{2})$  due to the time reversal symmetry. We can numerically calculate the quantity  $\chi_{\rho}(\mathbf{k})$  and then expand it around small momentum  $\mathbf{k}$  using Taylor series. This expansion leads to the coherence length  $\xi$ .

- 
- [1] Alexander Altland and Ben D Simons, *Condensed matter field theory* (Cambridge university press, 2010).
- [2] Nicola Marzari and David Vanderbilt, “Maximally localized generalized wannier functions for composite energy bands,” *Phys. Rev. B* **56**, 12847–12865 (1997).
- [3] Sebastiano Peotta and Päivi Törmä, “Superfluidity in topologically nontrivial flat bands,” *Nature Communications* **6**, 8944 (2015), [arXiv:1506.02815 \[cond-mat.supr-con\]](#).
- [4] Grigory Tarnopolsky, Alex Jura Kruchkov, and Ashvin Vishwanath, “Origin of Magic Angles in Twisted Bilayer Graphene,” *Phys. Rev. Lett.* **122**, 106405 (2019), [arXiv:1808.05250 \[cond-mat.str-el\]](#).
- [5] Jianpeng Liu, Junwei Liu, and Xi Dai, “Pseudo landau level representation of twisted bilayer graphene: Band topology and implications on the correlated insulating phase,” *Phys. Rev. B* **99**, 155415 (2019).
- [6] Douglas R. Hofstadter, “Energy levels and wave functions of bloch electrons in rational and irrational magnetic fields,” *Phys. Rev. B* **14**, 2239–2249 (1976).
- [7] Fenner Harper, Steven H. Simon, and Rahul Roy, “Perturbative approach to flat chern bands in the hofstadter model,” *Phys. Rev. B* **90**, 075104 (2014).
- [8] N. B. Kopnin and E. B. Sonin, “BCS Superconductivity of Dirac Electrons in Graphene Layers,” *Phys. Rev. Lett.* **100**, 246808 (2008), [arXiv:0803.3772 \[cond-mat.supr-con\]](#).
- [9] V. J. Kauppila, F. Aikebaier, and T. T. Heikkilä, “Flat-band superconductivity in strained dirac materials,” *Phys. Rev. B* **93**, 214505 (2016).
- [10] Teemu J. Peltonen and Tero T. Heikkilä, “Flat-band superconductivity in periodically strained graphene: mean-field and Berezinskii-Kosterlitz-Thouless transition,” *Journal of Physics Condensed Matter* **32**, 365603 (2020), [arXiv:1910.06671 \[cond-mat.supr-con\]](#).
- [11] Roger A Horn and Charles R Johnson, *Matrix analysis* (Cambridge university press, 2012).
- [12] Tomoki Ozawa and Bruno Mera, “Relations between topology and the quantum metric for Chern insulators,” *Phys. Rev. B* **104**, 045103 (2021), [arXiv:2103.11582 \[cond-mat.mes-hall\]](#).
- [13] Haidong Tian, Xueshi Gao, Yuxin Zhang, Shi Che, Tianyi Xu, Patrick Cheung, Kenji Watanabe, Takashi Taniguchi, Mohit Randeria, Fan Zhang, Chun Ning Lau, and Marc W. Bockrath, “Evidence for Dirac flat band superconductivity enabled by quantum geometry,” *Nature (London)* **614**, 440–444 (2023).
- [14] Rafi Bistritzer and Allan H. MacDonald, “Moiré bands in twisted double-layer graphene,” *Proceedings of the National Academy of Science* **108**, 12233–12237 (2011), [arXiv:1009.4203 \[cond-mat.mes-hall\]](#).
- [15] Mikito Koshino, Noah F. Q. Yuan, Takashi Koretsune, Masayuki Ochi, Kazuhiko Kuroki, and Liang Fu, “Maximally localized wannier orbitals and the extended hubbard model for twisted bilayer graphene,” *Phys. Rev. X* **8**, 031087 (2018).
- [16] A. Julku, T. J. Peltonen, L. Liang, T. T. Heikkilä, and P. Törmä, “Superfluid weight and berezinskii-kosterlitz-thouless transition temperature of twisted bilayer graphene,” *Phys. Rev. B* **101**, 060505 (2020).
- [17] Xiang Hu, Timo Hyart, Dmitry I. Pikulin, and Enrico Rossi, “Geometric and conventional contribution to the superfluid weight in twisted bilayer graphene,” *Phys. Rev. Lett.* **123**, 237002 (2019).